THE JOURNAL OF CHEMICAL PHYSICS

VOLUME 11 NUMBER 7

JULY, 1943

Published by the
AMERICAN INSTITUTE OF PHYSICS
Incorporated
LANCASTER, PA., AND NEW YORK, N. Y.

THE JOURNAL OF CHEMICAL PHYSICS

ADVISORY EDITORIAL BOARD

R. T. Birge
A. H. Compton
James Franck
Irving Langmuir
John T. Tate
Harold C. Urey

BOARD OF EDITORS

Joseph E. Mayer, *Editor*

Associate Editors

Term ending December 31, 1943

Simon Freed
Maurice L. Huggins
J. G. Kirkwood
George Scatchard
J. H. Van Vleck

Term ending December 31, 1944

Charles O. Beckman
Bryce L. Crawford, Jr.
P. Debye
David Harker
Frank H. Westheimer

Term ending December 31, 1945

L. O. Brockway
Ronald W. Gurney
Kenneth S. Pitzer
Alfred L. Sklar
E. W. R. Steacie
Hugh S. Taylor

THE JOURNAL OF CHEMICAL PHYSICS is published monthly by the American Institute of Physics. Its purpose is to bridge a gap between journals of physics and journals of chemistry. The artificial boundary between physics and chemistry has now been in actual fact completely eliminated, and a large and active group is engaged in research which is as much the one as the other. It is to this group that the Journal is rendering its principal service and makes its greatest appeal, both as a prompt and efficient medium for publication of research and as a convenient and carefully edited assemblage of pertinent information.

Manuscripts for publication should be submitted to Joseph E. Mayer, Hitchcock Hall, Columbia University, New York, New York.

Reprint and all correspondence concerning papers in the process of publication should be addressed to the Publication Manager, American Institute of Physics, 175 Fifth Avenue, New York, New York.

Subscriptions and orders for single copies should be addressed to Prince and Lemon Streets, Lancaster, Pennsylvania, or to the American Institute of Physics, 175 Fifth Avenue, New York, New York.

Change of address should be addressed to the Publication Manager.

Subscription Price

The United States and Possessions, Canada and Mexico $10.00
Elsewhere 11.00

Back Numbers

Complete set: Vol. 1, 1933—Vol. 10, 1942 ..... $100.00
Yearly rate: $11.00.
Single copies: $1.00 each.

The Journal of Chemical Physics is published monthly at Prince and Lemon Streets, Lancaster, Pennsylvania.

Entered as second-class matter December 20, 1932, at the Post Office at Lancaster, Pa., under the Act of August 24, 1912. Acceptance for mailing at special rate of postage, provided for in the Act of February 28, 1925, embodied in paragraph 4, Section 412, P. L. & R., authorized

THE JOURNAL
OF
CHEMICAL PHYSICS

VOLUME 11, NUMBER 7 JULY, 1943

Raman Spectra of Hydrocarbons

III. Diisobutylene, Cyclohexene, and Dipentene

FORREST F. CLEVELAND
Department of Physics, Illinois Institute of Technology, Chicago, Illinois

(Received May 12, 1943)

Raman frequencies, relative intensities, and depolarization factors are listed for diisobutylene, cyclohexene, and dipentene. The relative intensities and depolarization factors were obtained with the aid of a Gaertner microdensitometer. The results are compared with data previously obtained for six olefins containing the groups XHC=CH_2, XYC=CH_2, or XHC=CHY (*trans*). The present compounds contain the groups XYC=CH_2, XHC=CHX (*cis*), and XYC=CHZ. The first of these has nearly the same olefinic frequencies previously found for 2-methyl-1-heptene, except that the 1414 cm^{-1} frequency of the latter has dropped to 1376. The last two groups were contained in the similar ring structures of cyclohexene and dipentene and had nearly the same frequencies, except that the 1653 and 3023 cm^{-1} frequencies for XHC=CHX (*cis*) appeared at 1682 and 3012 for XYC=CHZ. Previous data for the three compounds are collected and compared with the present results. Lack of agreement between the present results in the 1100 and 3000 cm^{-1} region for diisobutylene and the previous data for 2,4,4-trimethyl-1-pentene is attributed to incorrect assignment of the exciting lines in the previous work.

INTRODUCTION

DOUBLE-BONDS in hydrocarbons have associated with them a definite set of Raman frequencies, the number and position of which depends upon the nature of the substitutions at the ethylenic carbon atoms. The first two papers[1,2] of this series gave the results of investigations of straight and branched chain olefins containing eight carbon atoms and containing the groups XHC=CH_2, XYC=CH_2, or XHC=CHY (*trans*). The present paper is a report of the results of an investigation of the Raman spectra of diisobutylene, a branched chain olefin containing eight carbon atoms and containing principally the group XYC=CH_2; cyclohexene, an olefin which contains the group XHC=CHX (*cis*); and dipentene, a diolefin which has a ring structure identical with that of cyclohexene and which may be derived from the latter by substitution of a methyl and propylene group for the hydrogens in the 1- and 4-positions, respectively, the double bond being at the 1-position. The dipentene contains the groups XYC=CH_2 and XYC=CHZ. It will be interesting to compare the olefinic frequencies of the groups which are the same as those in the prior investigations with the values there obtained and to observe what olefinic frequencies are associated with the new groups, although it is to be expected that the situation may be changed somewhat by the presence of ring structures rather than the open chains of the previously investigated compounds.

EXPERIMENTAL

The apparatus and experimental technique were described in the previous papers.[1,2] The

[1] Forrest F. Cleveland, J. Chem. Phys. **11**, 1 (1943).
[2] Forrest F. Cleveland, J. Chem. Phys. **11**, 227 (1943).

spectrograms were made with the samples in the liquid state and excitation was exclusively by Hg 4358A. The physical properties of the materials were as follows:

Diisobutylene,

$$(CH_3)_3CHC{=}C(CH_3)_2,$$

and

$$(CH_3)_3CCH_2(CH_3)C{=}CH_2,$$

C_8H_{16}: m. p. −102.4 to −111.6°C; b. p. 102.25°C; n_D^{20}, 1.4102; d_4^{20}, 0.7166.

Cyclohexene,

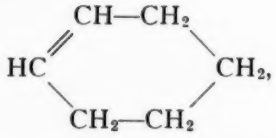

C_6H_{10}: m. p. −103.66°C; b. p. 83.19°C; n_D^{20}, 1.4467; d_4^{20}, 0.8107.

Dipentene,

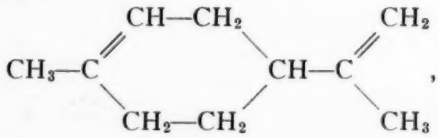

$C_{10}H_{16}$: m. p. −95.5°C; b. p. 176.6°C; n_D^{20}, 1.4739 to 1.4740; d_4^{20}, 0.8446.

RESULTS

Diisobutylene

Diisobutylene is a mixture of 2,4,4-trimethyl-1-pentene and 2,4,4-trimethyl-2-pentene which has been separated into its components in only one investigation.[3] Fortunately the Raman frequencies and estimated intensities of the separated isomers were obtained[4] and the availability of these data facilitates the interpretation of the results obtained in the present investigation. From the physical properties, the present sample was expected to contain about 85 percent of the 2,4,4-trimethyl-1-pentene and the spectroscopic results bear out this expectation. Depolarization factors are obtained for the first time and the relative intensities are more precise than those previously reported.

[3] F. C. Whitmore and S. N. Wrenn, J. Am. Chem. Soc. **53**, 3136 (1931).
[4] D. H. Rank and E. R. Bordner, J. Chem. Phys. **3**, 248 (1935).

The present results for diisobutylene are compared with the previous data for 2,4,4-trimethyl-1-pentene and 2,4,4-trimethyl-2-pentene in Table I. Examination of the table shows that the spectrum of the present sample of diisobutylene is nearly identical with that of 2,4,4-trimethyl-1-pentene; several strong lines in the spectrum

TABLE I. Comparison of the Raman data for diisobutylene with the previous data for 2,4,4-trimethyl-1-pentene and 2,4,4-trimethyl-2-pentene.

2,4,4-Trimethyl-1-pentene		Diisobutylene			2,4,4-Trimethyl-2-pentene	
$\Delta\nu$	I_e	$\Delta\nu$	I	ρ	$\Delta\nu$	I_e
124	4b	124	184	0.68		
					133	2b
190	2	189	60	0.39		
					202	2
294	4	287	95	0.54		
					300	2
315	4	314	59	0.57		
					327	8
387	4	383	64	0.40		
		416	30	0.71		
461	2	458	17	0.60		
		498	vw		506	2
561	10	559	109	0.15		
					568	8
685	15	685	165	0.07		
765	20	766	250	0.13	760	20
					820	4
829	6	825	43	0.24		
894	4	890	77	0.52		
910	8	908	121	0.64		
					924	10
936	8	932	108	0.63		
					940	2
		970	vw			
		997	vw			
999	2				1027	4
1049	2					
					1071	6
1101	2					
1155	8	1151	64	0.52	1159	4
1207	6	1199	59	0.66	1204	6
1240	10	1236	104	0.63		
					1257	4
1268	2	1264	vw			
1297	2	1295	vw			
1328	2	1324	vw			
					1357	4
		1383	vw		1386	10
					1395	6
1413	15	1410	155	0.62		
1450	12b	1448	268	0.88	1450	15
		1462	124	0.78	1466	8
1648	15	1644	161	0.33		
		1658	51	P	1667	15
		2866	228	0.22		
2906	6	2907	1000	0.18	2903	10
2947	10b	2956	980	0.76	2948	15b
		2977	790	P		
2996	10				3000	15b
3021	6	3072	32	0.71		

$\Delta\nu$ is the Raman frequency in cm^{-1}, I_e is the estimated relative intensity, I is the relative intensity obtained with the aid of the microdensitometer, ρ is the depolarization factor, b indicates unusually broad lines, and vw (very weak) indicates lines that were too weak to measure with the microdensitometer.

of 2,4,4-trimethyl-2-pentene, notably those at 327, 568, 924, 1071, 1257, 1357, and 1395, do not appear in the diisobutylene spectrum. The first six lines in the 2,4,4-trimethyl-2-pentene spectrum appear at slightly higher frequencies than the corresponding lines in the 2,4,4-trimethyl-1-pentene spectrum. The strong, polarized line occurring in the three spectra near 764 cm^{-1} is the line characteristic of the neopentyl group $(CH_3)_3C-$; it occurs in this region for a great variety of compounds and is always highly polarized. The line observed for diisobutylene at 1383 and probably also the one at 1658 owe their existence to the presence of the small amount of 2,4,4-trimethyl-2-pentene; one cannot be sure about the latter because the branched chain olefins, 2-methyl-1-heptene and 6-methyl-1-heptene, gave two lines in the 1650 cm^{-1} region. However, since only one line was observed for 2,4,4-trimethyl-1-pentene by Rank and Bordner,[4] it seems probable that the 1658 line is due to the presence of the 2,4,4-trimethyl-2-pentene.

Since the principal component of the diisobutylene contained the group $XYC=CH_2$, one might expect to obtain the same set of olefinic frequencies as that obtained previously for 2-methyl-1-heptene. The corresponding data are compared in Table IV; the frequencies are nearly the same, but the 1653, 1674 doublet in 2-methyl-1-heptene has dropped to 1644, 1658[5] and the 1295 line is very weak.

The agreement between the present results and those of the previous investigation[4] is not very good in the 1100 and 3000 cm^{-1} region; the lines found at 2866, 2977, and 3072 in the present study were not found previously, while the lines previously observed at 1049, 1101, 2996, and 3021 were not found. These discrepancies seem to be due to incorrect assignment of the exciting lines; for 1101*e* could be 2868*k*, 1049*k* could be 1238*i*, 1207*e* could be 2974*k*, 2996*k* could be 1229*e*, and 3021*e* could be 2964*f* ($k=4047$, $i=4078$, $f=4348$, $e=4358$A). If these changes are made, the two spectra are in agreement. It is possible that similar errors due to use of the wrong exciting line may be present in the data listed[4] for the 2,4,4-trimethyl-2-pentene; hence the Raman spectrum of this compound should be reinvestigated.

[5] Assuming for the moment that this line might be due to the 2,4,4-trimethyl-1-pentene.

TABLE II. Comparison of present and previous results for the Raman spectrum of cyclohexene.

Cyclohexene								Cyclohexane*		
	Previous data				Present results					
N	$\Delta\nu$	d	I_e	ρ	$\Delta\nu$	I	ρ	$\Delta\nu$	I_e	
5	175	2	2	D	±175	84	0.68			
5	281	6	3	D	±279	80	0.84			
6	394	2	5	D	±395	202	0.41	380	1/2	
4	450	2	2	D	453	34	0.65	425	1	
5	492	2	2		493	28	0.61			
5	642	4	1		640	22	0.74			
5	714	9	2		718	16	0.23	695	0	
7	823	3	8	P	±824	980	0.14	801	10	0.06
5	875	2	2		875	33	0.90			
5	904	1	3		904	41	0.23			
5	966	2	3		964	29	0.61			
1	997		8	pP				992	0?	
6	1034	3	3		1039	60	0.59	1028	8	0.70
7	1066	4	5	pP	1068	180	0.64			
4	1138	2	1		1139	16	0.41	1158	1	
7	1219	2	6	D	1222	407	0.47			
4	1244	3	2		1241	81	0.64			
7	1267	5	4	D	1266	111	0.75	1266	5	0.70
3	1344	2	3	pP	1343	29	0.61	1344	1/2	P
7	1430	3	7	D	1433	710	0.55	1442	5	D
5	1454	7	4	D	1453	230	0.65	2351	0	
7	1650	3	7	P	1653	447	0.14	2462	0	
1	2634		9		2638	9		2628	0	
1	2660		1		2659	11		2662	1	
					2695	vw		2694	1/2	
6	2828	9	7		2836	532	0.20	2853	8	0.10
6	2864	4	5		2867	690	0.41			
3	2880	5	5					2887	1	D
7	2912	3	7		2910	1000	0.33	2922	8	D
6	2939	3	7		2937	890	0.25	2935	8	P
6	3020	6	6		3023	508	0.19			
					3059	19	D			

N is the number of times a line has been observed previously in separate investigations, d is the mean deviation of the Raman frequency, P = polarized, pP = partially polarized, D = depolarized, ± means that the line was observed both as a Stokes and as an anti-Stokes line.

* Data from M. Magat, *Tables Annuelles de Constantes et Données Numériques, Effet Raman* (Gauthier-Villars, Paris, 1936), Vol. 11, p. 52.

Cyclohexene

Raman frequencies and estimated intensities for cyclohexene have been obtained by several investigators,[6-13] but polarization data, qualitative and incomplete, have been reported only

[6] R. Lespieau and M. Bourguel, Bull. Soc. Chim. **47**, 1365 (1930).
[7] C. S. Morris, Phys. Rev. **38**, 141 (1931).
[8] J. Weiler, Zeits. f. Physik **69**, 586 (1931).
[9] R. W. Wood and G. Collins, Phys. Rev. **42**, 386 (1932).
[10] M. Godchot, E. Canals, and G. Cauquil, Comptes rendus **196**, 780 (1933).
[11] E. Canals, M. Mousseron, L. Souche, and P. Peyrot, Comptes rendus **202**, 1519 (1936).
[12] K. W. F. Kohlrausch and R. Seka, Ber. **69**, 729 (1936).
[13] H. J. Taufen, M. J. Murray, and Forrest F. Cleveland, J. Am. Chem. Soc. **63**, 3500 (1941).

once.[14] The present report gives new frequency measurements, more precise relative intensities, and quantitative depolarization factors. The results are compared with the previous data in Table II. The values listed under $\Delta\nu$ and I_e of the previous data column are the mean values for the previous investigations. The intensity of 9 reported by Wood and Collins[9] for the 2634 cm^{-1} line must be an error, for the intensity of this line in the present investigation was less than that of the 2660 line to which they give an intensity value of 1; the most intense line reported by them was given an intensity value of 10. New lines were observed at 2695 and 3059 cm^{-1}.

TABLE III. Comparison of the present results for dipentene with previous data for dipentene and limonene.

Previous data: Limonene				Previous data: Dipentene				Present results: Dipentene		
N	$\Delta\nu$	d	I_e	N	$\Delta\nu$	d	I_e	$\Delta\nu$	I	ρ
								176	80	0.95
								196	21	
								256	vw	
2	312	4	1	1	307		2	305	103	0.63
1	330		2	1	330		2	337	87	0.87
1	350		1							
4	432	2	2	2	425	1	2	426	55	0.70
1	470		1	1	447		1	444	20	0.48
3	491	4	2	1	492		2	492	13	0.53
1	503	0		1	509		1			
4	523	3	3	1	521		2	520	25	0.69
3	548	3	2	1	542		2	545	32	0.47
				1	569		1			
3	640	2	1	3	636	3	3	642	44	0.75
1	662		1	2	671	3	1			
3	705	4	1	3	707	5	2	697	21	
4	760	5	6	2	757	3	4	760	170	0.37
2	788	1	3	2	792	3	3			
3	801	1	4	2	804	3	3	799	146	0.39
				2	817	1	1	815	34	
4	893	4	3	2	875	4	4	886	47	0.85
3	915	2	1	2	918	1	3	916	16	0.20
1	927		4	1	934		1			
3	956	0	1	2	950	2	2	955	4	
1	995		1							
4	1020	2	2	1	1013		0	1017	22	0.45
4	1064	7	2	2	1047	4	2	1056	36	0.46
								1079	29	0.62
4	1089	7	2	1	1096		2	1109	22	0.47
3	1120	3	2							
4	1158	5	4	2	1153	5	3	1156	49	0.27
								1186	22	D
4	1205	4	1	2	1206	1	3	1209	89	0.41
				1	1227		2			
3	1246	4	1					1246	26	D
4	1287	4	2	3	1295	8	3	1290	46	0.72
4	1312	4	2					1311	54	0.73
1	1333		2							
4	1372	4	5	3	1369	4	4			
1	1380		5	1	1377		7	1376	127	0.70
1	1397		2							
3	1433	2	11	1	1429		3	1437	461	0.61
2	1454	1	10	2	1442	2	3	1454	210	0.69
				1	1508		2			
				1	1549		3			
				2	1609	2	8	1617	40	0.78
3	1645	1	12	2	1642	4	5	1648	213	0.38
1	1658		3	1	1658		3			
4	1676	5	10	3	1676	2	5	1682	219	0.35
				1	2661		0			
				1	2722		0	2725	5	
3	2834	1	4	1	2820		1	2834	179	0.33
2	2858	2	2							
2	2881	1	5	2	2868	1	3	2868	414	0.35
3	2913	3	6							
3	2926	3	6	2	2919	3	3	2915	1000	0.30
4	2966	5	3	2	2969	2	3	2964	292	0.62
1	2981		4					2983	115	P
2	3014	4	2					3012	54	P
2	3046	2	5	1	3047		4	3050	26	D
3	3082	0	2					3078	16	D
1	(3156)									

The cyclohexene molecule contains the group XHC=CHX (*cis*), although the situation is complicated by the fact that the two X groups are joined together to give a cyclic molecule. The olefinic frequencies associated with this group in cyclohexene are compared with the olefinic frequencies for the other groups in Table IV. It is especially appropriate to compare this set of frequencies with those previously obtained for olefins containing the group XHC=CHY (*trans*); the depolarized line observed near 3075 for many olefins and which was not found in the spectra of olefins containing the XHC=CHY (*trans*) group appeared at 3059 cm^{-1} for cyclohexene. All the other frequencies appeared at lower values than in the olefins containing the XHC=CHY (*trans*) group, except the 3023 line which appeared with a higher frequency. Corresponding olefinic frequencies for *cis*-2-hexene[15] are 1259(5) or 1299(2), 1658(7), and 3017(6) and for *cis*-2-butene they are[13] 1253(8), 1660(10), and 3023(9).

It is interesting to compare the cyclohexene spectrum with that of cyclohexane. The data for the latter are listed in Table II. Many of the frequencies are nearly the same in the two spectra; notable exceptions are the cyclohexene lines at 175, 279, 453, 493, 875, 904, 964, 1068, 1139, 1222, and 1241, in addition to the olefinic frequencies mentioned above. The strong cyclohexene line at 1222 cm^{-1} is especially outstanding. It does not appear in the spectrum of *cis*-2-hexene.[15] The strong, highly polarized, ring frequency at 801 in cyclohexane appears at 824 in cyclohexene.

[14] E. Canals, M. Mousseron, L. Souche, and P. Peyrot, Bull. Soc. Chim. **5**, 79 (1938).

[15] B. Gredy, Bull. Soc. Chim. **2**, 1029 (1935).

Dipentene

Raman frequencies and estimated intensities have been reported previously for both dipentene[16–18] and limonene,[6,17,19–21] but no polarization data seem to have been reported. The present results for dipentene are compared with the data previously reported for dipentene and limonene in Table III.[22] Dipentene or *dl*-limonene is the racemic form of limonene. The molecule consists of a cyclohexene ring with a methyl group substituted for one of the ethylenic hydrogens and with an isopropylene group substituted for one of the hydrogens in the position *para* to the methyl group. It may thus be called 1-methyl-4-isopropylene-1-cyclohexene. There is a double bond in the ring and one outside the ring, in the isopropylene group. One might expect that the olefinic frequencies associated with the ring double bond would have values close to those for cyclohexene; the corresponding data are compared in Table IV, the ring double bond frequencies being those for the group XYC=CHZ. The drop of the 3023 frequency in cyclohexene to 3012 in dipentene is in line with a similar drop observed in the previous investigation[2] for 2-methyl-1-heptene; there it was found that the frequency at 3001 cm^{-1} in 6-methyl-1-heptene dropped to 2978 in 2-methyl-1-heptene. Both the 2-methyl-1-heptene and dipentene for which the lower frequencies were observed have one ethylenic carbon with no attached hydrogen atoms. Also the increase of the 1653 cyclohexene frequency to 1682 in dipentene is analogous to the increase of the 1644 6-methyl-1-heptene frequency to 1653 in 2-methyl-1-heptene.

The group corresponding to the double bond outside the ring in dipentene is $XYC=CH_2$. The frequencies attributed to this group (see Table IV) are very nearly the same as those for 2-methyl-1-heptene, except for the 1376 line which has a much lower value in dipentene. The line at 1617 cm^{-1} in the dipentene spectrum is probably due to the presence of α-terpinene[17] in the sample of dipentene; this would account for the fact that the dipentene sample appeared to be slightly low in melting point, boiling point, and density. From the results for the other olefins one would expect this line to be strongly polarized; on the contrary it appears to be depolarized. It seems likely that only two of the six lines observed by Jatkar and Padmanabhan[17] for dipentene in the region 1500 to 1700 cm^{-1} were due to the dipentene molecule, the others probably being due to the presence of impurities.

Examination of Table III shows that the agreement between the present and previous results is not as good as usual for Raman spectra of organic compounds made in different laboratories. The reason for this is no doubt to be found in the presence of impurities in the samples used in obtaining the spectra in the different investigations. By and large, there is little difference in the spectra for dipentene and limonene. This is in line with the fact that Mr. G. V. Nevgi[17] found no difference in the Raman spectra of *d*- and *l*-limonenes.

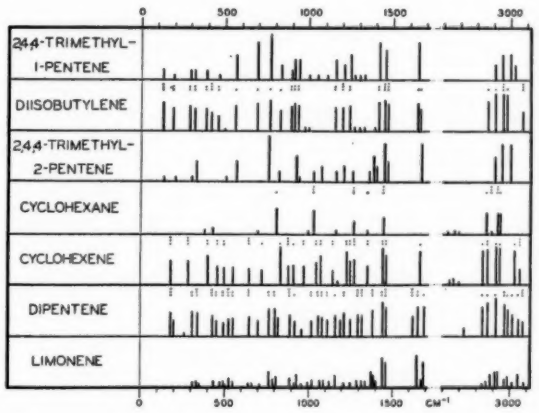

FIG. 1. Comparison of the present Raman data for diisobutylene with that for 2,4,4-trimethyl-1-pentene and 2,4,4-trimethyl-2-pentene and of the present Raman data for cyclohexene and dipentene with that for cyclohexane and limonene.

CONCLUSION

A graphical over-view of the data is given in Fig. 1; in the upper part of the figure, the

[16] P. S. Srinivasan, Indian Acad. Sci. **A2**, 105 (1935).
[17] S. K. K. Jatkar and R. Padmanabhan, Indian J. Phys. **10**, 55 (1936).
[18] G. Dupont, J. Levy, and M. Marot, Bull. Soc. Chim. **53**, 393 (1933).
[19] A. Kastler, Comptes rendus **191**, 565 (1930).
[20] G. B. Bonino and P. Cella, Mem. accad. Italia, Chim. **2**, 5 (1931).
[21] G. Dupont, P. Daure, and J. Levy, Bull. Soc. Chim. **51**, 921 (1932).
[22] Results obtained in seven separate investigations for dipentene or limonene are tabulated side by side for comparison in a paper by W. R. Angus, *Raman Jubilee Volume* (Indian Acad. Sciences, 1938), p. 529.

TABLE IV. Comparison of the olefinic frequencies for different groups.

							$H_2C=CH_2$								
Ethylene*			1341	St.**	0.17		1619	St.	P	3009	St.	0.10	3075	—	—
							$XHC=CH_2$								
1-Octene	1293	94	0.88	1415	42	0.77	1641	134	0.15	2999	124	0.28	3078	23	0.93
6-Methyl-1-heptene	1295	212	0.45	1417	112	0.56	1644	342	0.19	3001	228	0.27	3079	70	0.73
							1672	vw							
							$XYC=CH_2$								
2-Methyl-1-heptene	1303	52	0.64	1414	108	0.81	1653	203	0.20	2978	253	P	3077	47	0.70
							1674	55	P						
2,4,4-Trimethyl-1-pentene	1295	vw	—	1410	155	0.62	1644	161	0.33	2977	790	P	3072	32	0.71
							(1658	51	P)						
Dipentene	1290	46	0.72	1376	127	0.70	1648	213	0.38	2983	115	P	3078	16	D
	1311	54	0.73												
							XHC=CHY (*trans*)								
2-Octene	1300	40	0.64	—	—	—	1672	47	0.23	3004	37	0.34	—	—	—
3-Octene	1303	87	0.56	—	—	—	1672	173	0.16	2998	59	0.29	—	—	—
4-Octene	1290	41	0.54	—	—	—	1672	150	0.19	2997	27	0.36	—	—	—
							XHC=CHX (*cis*)								
Cyclohexene	1241	81	0.64	—	—	—	1653	447	0.14	3023	508	0.19	3059	19	D
							XYC=CHZ								
Dipentene	1246	26	D	—	—	—	1682	219	0.35	3012	54	P	3050	26	D

* Data from M. Magat, *Tables Annuelles de Constantes et Données Numériques, Effet Raman* (Hermann et Cie, Paris, 1937), Vol. 12, p. 53.
** St. =strong.

Raman data for diisobutylene are compared with that obtained by Rank and Bordner[4] for 2,4,4-trimethyl-1-pentene and 2,4,4-trimethyl-2-pentene. It is clear from the figure that the major portion of the diisobutylene sample was 2,4,4-trimethyl-1-pentene. In the lower part of the figure, the present results for cyclohexene and dipentene are compared with previous results for cyclohexane and limonene. For diisobutylene, cyclohexene, and dipentene the height of the line is proportional to the logarithm of the relative intensity obtained with the microdensitometer; for the other compounds, the height of the line is proportional to the estimated intensity. The dots above the lines indicate the state of polarization, single dots for $\rho<0.35$, double dots for $0.35\leq\rho\leq0.65$, and triple dots for $\rho>0.65$.

The olefinic frequencies for the various groups are collected for comparison in Table IV. The choice of the line near 1300 cm^{-1} is to some extent arbitrary since it is not constant in frequency and since there are other lines in the neighborhood. It must be remembered that the intensities can be only qualitatively compared in the several spectra, because for each spectrum the intensities are relative to the strongest Raman line in that spectrum.

ACKNOWLEDGMENT

The hydrocarbons used in this work were prepared under the direction of Professor C. E. Boord of the Department of Chemistry of the Ohio State University as part of the American Petroleum Institute Hydrocarbon Research Project in the Industrial Research Foundation of the University. The microdensitometer used in the intensity measurements was obtained with a grant made to the author from the Penrose Fund of the American Philosophical Society. The Hilger spectrograph was obtained, in part, with a grant made to the author from the Permanent Science Fund of the American Academy of Arts and Sciences. The author wishes to express his appreciation for this assistance.

The Low Velocity Scattering of H^+ and H_3^+ in Hydrogen

J. H. SIMONS, C. M. FONTANA, E. E. MUSCHLITZ, JR., AND S. R. JACKSON
School of Chemistry and Physics, The Pennsylvania State College, State College, Pennsylvania

(Received February 2, 1943)

The theory of the elastic scattering of a low velocity ion in a gas is examined in some detail. More precise measurements are reported on the elastic scattering of H^+ and H_3^+ in hydrogen in the velocity range of 2 to 135 volts. The simple exponential form of a potential law is shown to change with the velocity of the ion, i.e., with distance of closest approach of the interacting particles. For H^+ in H_2 this is—

$$V=-\frac{20.37\times10^{-32}}{r^4} \text{ from 2 to 24 volts } (r_a>1.74\text{A})$$

and

$$V=-\frac{8.68\times10^{-14}}{r^{1.74}} \text{ from 24 to 135 volts } (r_a=1.74 \text{ to } 1.5\text{A}).$$

The interaction energy calculated on this basis is 3.0 electron volts instead of the 3.5 previously reported. For H_3^+ in H_2 an average taken from 5.4 to 130 volts is

$$V=-\frac{1.145\times10^{-36}}{r^{4.60}} \quad (r_a=2.12 \text{ to } 1.07\text{A});$$

but between 10.5 and 28 volts ($r_a=1.85$ to 1.48A)

$$V=-\frac{5.98\times10^{-32}}{r^4}.$$

Both inverse fourth-power potential laws are compared with a similar law evaluated on the basis of the interaction being due solely to that of the charge on the ion interacting with the induced dipole of the hydrogen molecule. The H_3^+ law is seen to approximate this closely whereas the H^+ law does not.

IN a previous paper[1] the need for more precise hydrogen ion scattering measurements was emphasized. A new apparatus has been constructed and described in a recent article.[2] We can now report elastic scattering measurements of H^+ and H_3^+ in molecular hydrogen which are sufficiently precise to show a variation of force law with distance.

The analytical treatment for the determination of force laws from the scattering data is examined and the assumptions involved in a general approximate treatment of the scattering problem are discussed.

ANALYSIS

To evaluate a potential law,

$$V=-K/r^n \tag{1}$$

between the ion and the gas molecule from the measurements obtained and the constants of the apparatus, the procedure used is to examine the angular change in direction of the ion due to this interaction and integrate this for the full length of the scattering cylinder. This is necessary as the angle that the ion needs to be bent to be counted as scattered in the apparatus increases as the collision takes place nearer and nearer the exit hole of the scattering cylinder. For the general solution of this problem a number of commonly used assumptions are employed. One of these is that the mass of the molecule is large compared to that of the ion. The error introduced by this assumption is herein examined.

The value of n, the exponent of r in the potential law, as given in the general approximate treatment and obtained directly from the scattering measurements is identical with the value given by more exact and rigorous analyses of the problem which can be made for specific whole number values of n and for specified mass ratios, m_1/m_2. The numerical value of the constant, K, is obtained from the scattering measurements and the dimensions of the apparatus; but different values result from the use of equations derived from the general or exact analysis. In a later paper[3] the exact treatment will be given for the cases $n=0$, 1, 2, and 4 and a method presented for correcting the values of K obtained by the general treatment. This enables accurate values of K to be obtained from the general treatment for fractional values of n.

[1] A. S. Russell, C. M. Fontana, and J. H. Simons, J. Chem. Phys. **9**, 381 (1941).
[2] J. H. Simons, H. T. Francis, C. M. Fontana, and S. R. Jackson, Rev. Sci. Inst. **13**, 419 (1942).
[3] J. H. Simons, E. E. Muschlitz, Jr., and L. G. Unger, "The scattering of low velocity hydrogen ions in helium," p. 322, this issue.

The scattering takes place in a cylinder of length, l. The ions enter through a hole in the center of one end of this cylinder and the unscattered ones leave by a hole of radius, a, in the center of the other end. These are then collected in a Faraday cage, whereas the scattered ions are collected on the walls of the scattering cylinder. If the apparatus is in perfect alignment and the gas pressure is zero, all the ions entering this cylinder will leave through the exit hole, as this is larger than the entering hole and the beam is collimated. The total decrement dI_T of the beam current for any infinitesimal dx of the path length is given by:

$$dI_T = INP\pi r_0^2 dx, \tag{2}$$

where I is the beam current at point x.

N is the number of gas molecules per cc at 0°C and one mm pressure $= 3.536 \times 10^{16}$.

P is the pressure of the gas in mm at 0°C.

r_0 is the distance of closest approach between ion and molecule that will result in scattering through an angle, ϕ, which is the minimum angle of deflection which will result in the ion being counted as scattered, and r_a is the average value of r_0 for the length of the cylinder.

If α is the effective cross-sectional area of N molecules,

$$\alpha = N\pi r_a^2 = \frac{\int_0^l N\pi r_0^2 dx}{\int_0^l dx}. \tag{3}$$

Since

$$I = I_0 - I_T, \tag{4}$$

where I_0 is the initial beam current and I_T is the amount scattered up to point x,

$$\int_0^{I_T} \frac{dI_T}{I_0 - I_T} = \int_0^l P\alpha dx.$$

$$\ln \frac{I_0}{I_0 - I_T} = \ln \frac{I_0}{I_c} = \ln \frac{1}{R} = P\alpha l,$$

where R is the ratio of the number of unscattered ions to the total number of ions. Thus,

$$\alpha = \frac{1}{Pl} \ln \frac{1}{R}. \tag{5}$$

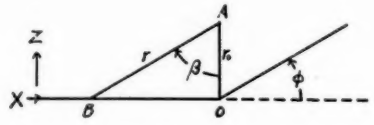

FIG. 1.

The use of Eq. (5) to calculate values of α is justified since values of $\log 1/R$ when plotted against P are found to be straight lines within the precision of the experiments.[1]

Consider an ion (Fig. 1) moving along X and in interaction with a molecule at A by the potential law, $V = -K/r^n$. Two assumptions will be used. The first is that the scattering angle, ϕ, is small and the second is that the mass of A is large compared to the mass of the ion; i.e., A is stationary. The force on the ion in the Z direction is:

$$F_z = \frac{nK}{r^{n+1}} \cos\beta = \frac{nK \cos^{n+2}\beta}{r_0^{n+1}}.$$

If U_x is the initial velocity in the X direction, U_z the resultant velocity in the Z direction, and t the time of travel between B and 0, then:

$$U_z = \frac{1}{m}\int_{-\infty}^{+\infty} F_z dt = \frac{2nK}{r_0^n m U_x}\int_{\beta=0}^{\beta=\pi/2} \cos^n \beta d\beta = \frac{2K}{mU_x r_0^n} C, \tag{6}$$

where

$$t = \frac{r_0}{U_x}\tan\beta, \quad dt = \frac{r_0}{U_x}\sec^2\beta d\beta$$

and

$$C = \frac{\pi^{\frac{1}{2}}\Gamma(\frac{1}{2}n + \frac{1}{2})}{\Gamma(\frac{1}{2}n)} \tag{7}$$

in terms of the gamma function, Γ.

The scattering angle ϕ is given by:

$$\tan\phi = \frac{U_z}{U_x} = \frac{2K_a C}{mU_x^2 r_0^n} = \frac{K_a C}{W r_0^n}, \tag{8}$$

where W is the initial kinetic energy of the ion measured in volts. The constant is now written as K_a to indicate that it arises from the above general approximate treatment.

This theory has been treated by Zwicky[4] but a derivation is given here as we wish to examine

[4] F. Zwicky, Physik. Zeits. **24**, 171 (1923).

the process further. For the minimum angle of scattering $\tan\phi = a/(l-x)$. From Eqs. (2) and (8)

$$dI_T = (I_0 - I_T)NP\pi\left[\frac{K_a C(l-x)}{Wa}\right]^{2/n} dx. \quad (9)$$

Integrating between 0 and l

$$\ln\frac{1}{R} = lP\alpha = \pi NP\left(\frac{K_a C}{Wa}\right)^{2/n}\frac{l^{2/n+1}}{2/n+1}. \quad (10)$$

$$\alpha = \frac{\pi}{2/n+1}N\left(\frac{K_a Cl}{Wa}\right)^{2/n}. \quad (11)$$

$$\alpha W^{2/n} = \frac{\pi}{2/n+1}N\left(\frac{K_a Cl}{a}\right)^{2/n} = Q. \quad (12)$$

The initial velocity of the ions in volts is W, and α is obtained from the scattering measurements by Eq. (5).

A plot of log α against log W will be a straight line, if Eq. (12) holds, and n is a constant. Q and n may then be obtained from the intercept and slope.

The desired constant, K_a, of the potential law, Eq. (1), is a function of Q, n, and the apparatus dimensions.

$$K_a = \left[\frac{Q(2/n+1)}{\pi N}\right]^{n/2}\frac{a}{lC}. \quad (13)$$

It will be shown later[3] that for more exact analyses with specific values of n the value of K will be a somewhat different function of the same quantities. A method of evaluating K from K_a will be given. In this, a multiplying factor, f, is found such that

$$K = fK_a. \quad (14)$$

The value of n, however, is identical in the more exact treatment with that in this general approximate treatment.

CONSIDERATION OF COMPARABLE MASSES

In the above, the assumption was made that the mass of the molecule was very large compared to the mass of the ion. The initial kinetic energy of the ion, W, appears, therefore, in Eq. (8). If, however, the molecule is of comparable mass to the ion, the scattering angle, ϕ, may be changed for two reasons. The velocity of the ion relative to the apparatus is affected by the exchange of kinetic energy between the colliding particles, and the angle of scattering relative to the apparatus is changed by the induced motion of the molecule. These effects are in the opposite direction. W is modified by the reduced mass $\mu = m_1m_2/(m_1+m_2)$. (m_1 is the mass of the ion and m_2 that of the molecule.)

$E = W(\mu/m_1)$. With the introduction of E the angle, θ, is the scattering angle relative to the molecule which is now moving. If ϕ is the angle of scattering relative to the apparatus,[5]

$$\cot\phi = \cot\theta + \frac{m_1}{m_2}\csc\theta. \quad (15)$$

This is obtained by consideration of the conservation of energy and momentum. For small angles of scattering, $\cot\theta = \csc\theta$, and Eq. (15) reduces to

$$\tan\theta = \frac{m_1}{\mu}\tan\phi; \quad (16)$$

but

$$\tan\theta = \frac{K_a C}{Er_0^n}, \quad \text{so} \quad \tan\phi = \frac{K_a C}{Wr_0^n}. \quad (17)$$

As Eq. (17) is identical with Eq. (8), it is seen that for small angles of scattering and for comparable masses, the tangent of the angle of scattering relative to the apparatus is related to the kinetic energy of the incoming ion by the same equation as derived for a stationary scattering molecule.

The foregoing analyses are approximate ones. The chief error is the simplification introduced by the assumption of a small angle of scattering. This occurs twice, once in the derivation of the general equation for a stationary scattering molecule and again in the correction for comparable masses of the particles. These errors tend to compensate but certainly will not do so completely in all cases. In particular, the initial assumption of a small scattering angle involves considerable error if n is large, for in this case the potential changes rapidly with distance resulting in scattering through larger angles.

---

[5] L. A. Pars, Phil. Mag. **33**, 96 (1942).

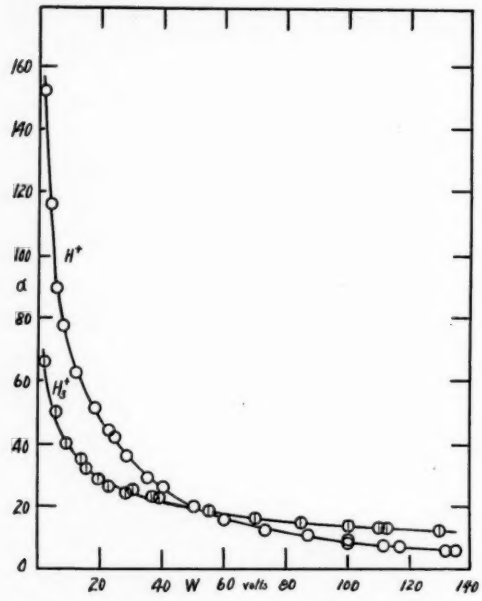

FIG. 2. The effective cross-sectional area of H_2 for scattering H^+ and H_3^+.

MEASUREMENTS

The measurements were made in the apparatus described elsewhere[2] and by the same technique. As the temperature of the scattering tube was different from 0°C, a correction for this was made. If the apparatus is in perfect alignment and it operates at zero pressure, all the ions will escape from the scattering cylinder; i.e., the "empty tube" ratio is one. As neither of these conditions are experimentally obtained, the difference between the scattering at two pressures is used in the calculations. If some low value of the pressure P_0 is used for one of these at which the scattering ratio R_0 is nearly one, the value of α can be obtained from the equation

$$\alpha=\frac{F}{P-P_0}\log\frac{R_0}{R}, \tag{18}$$

where

$$F=\frac{2.303(273.2+t°\mathrm{C})}{273.2l}, \tag{19}$$

and l for the present apparatus = 4.176 cm.

In Table I and Fig. 2 are shown the values of α as a function of W for H^+ scattered in H_2. From the logarithmic plot in Fig. 3 it is seen that the interaction can be represented as two potential laws. For velocities below 24 volts (r_a greater than 1.74A) an inverse fourth-power potential law results in which $Q=218$ and $K_a=26.95\times10^{-32}$ volt cm^4 calculated from the general approximate equation (13). By applying the correction factor, f, $K=20.37\times10^{-32}$ and

$$V=-\frac{20.37\times10^{-32}}{r^4}. \tag{20}$$

The average distance of closest approach r_a for any particular voltage, W, is obtained from the plot of the experimental values of α against voltage. From the value of α so found r_a is obtained from Eq. (3).

If it be considered that the interaction is solely that caused by the action of the charge of the ion with the induced dipole of the molecule, a potential function can be expressed using the assumption that r is large compared with the dipole distance.

$$V_p=-\alpha_p Z^2e^2/2r^4=-K_p/r^4, \tag{21}$$

where α_p is the polarizability of the molecule, e is the charge of an electron and Z is the number of charges on the ion. If the polarization, P_e of

TABLE I. The scattering of H^+ in hydrogen.

W Volts	$P\times10^4$ mm	$P_0\times10^4$ mm	R	R_0	F	α
1.70	30.30	0.20	0.160	0.898	0.6161	153
3.50	29.00	0.20	0.270	0.948	0.6161	117
5.50	29.00	0.20	0.378	1.000	0.6141	90.1
8.00	29.60	0.20	0.423	1.000	0.6161	78.3
12.0	29.50	0.20	0.501	1.000	0.6161	63.1
18.0	40.65	0.40	0.453	0.995	0.6100	51.8
22.6	29.73	0.20	0.610	1.000	0.6161	44.8
24.5	27.80	0.20	0.643	1.000	0.6151	42.7
29.0	38.67	0.40	0.587	0.995	0.6100	36.5
29.8	43.75	0.40	0.542	0.985	0.6060	36.3
35.0	29.65	0.20	0.718	0.990	0.6151	29.1
40.0	30.43	0.20	0.735	0.990	0.6161	26.4
45.0	29.04	0.20	0.775	0.992	0.6181	23.0
45.0	29.1	0.2	0.787	0.998	0.6161	22.0
50.0	29.1	0.2	0.800	0.995	0.6161	20.2
55.0	29.5	0.2	0.810	0.998	0.6161	19.1
60.0	29.1	0.2	0.838	0.998	0.6120	16.1
60.0	54.9	0.2	0.721	0.999	0.6100	15.8
60.0	56.25	0.25	0.719	0.998	0.6120	15.6
73.5	103.4	0.2	0.607	0.993	0.6120	12.7
87.0	70.4	0.4	0.751	0.995	0.6100	10.65
100.0	70.4	0.4	0.768	0.995	0.6100	9.78
100.0	103.4	0.2	0.704	0.993	0.6120	8.86
111.5	74.1	0.6	0.798	0.990	0.6120	7.80
117.0	103.4	0.2	0.740	0.993	0.6120	7.57
132.0	74.1	0.6	0.831	0.984	0.6120	6.11
135.0	105.2	0.20	0.772	0.993	0.6120	6.37

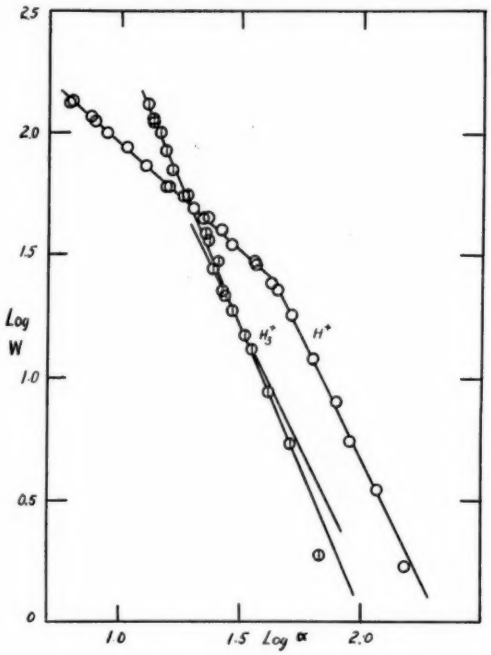

FIG. 3. H^+ and H_3^+ in H_2.

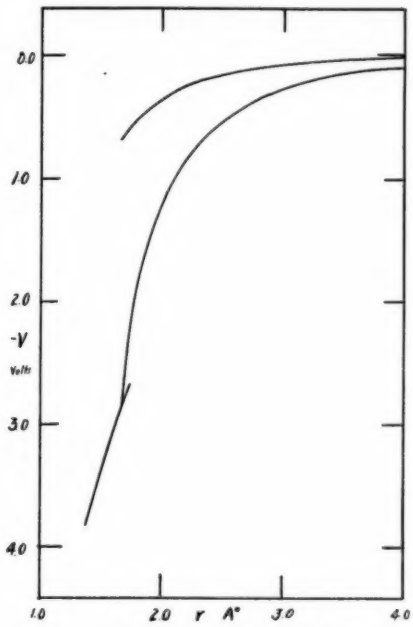

FIG. 4. Potential energy of H^+ and H_2. The upper curve represents the potential calculated on the basis of the interaction of the charge on the ion with the induced dipole of the molecule.

hydrogen is 2.0 cc per mole,

$$P_e=\frac{4}{3}\pi N_a\alpha_p \quad \text{or} \quad \alpha_p=7.88\times10^{-24}.$$

$$V_p=-\frac{5.64\times10^{-32}}{r^4}. \tag{22}$$

TABLE II. The scattering of H_3^+ in hydrogen.

W volts	$P\times10^3$ mm	$P_0\times10^3$ mm	R	R_0	F	α
1.90	25.6	0.2	0.222	0.418	0.6130	66.5
5.40	25.6	0.2	0.489	0.792	0.6141	50.6
8.80	25.6	0.2	0.618	0.916	0.6141	41.3
13.10	54.9	0.2	0.474	0.997	0.6161	35.4
15.0	55.15	0.20	0.507	0.995	0.6130	32.7
19.0	55.15	0.20	0.542	0.995	0.6130	29.4
21.5	55.2	0.2	0.563	0.987	0.6161	27.3
22.7	29.0	0.2	0.721	0.960	0.6161	26.6
28.0	55.15	0.20	0.600	0.995	0.6130	24.3
30.0	39.4	0.4	0.681	0.990	0.6100	25.4
36.4	55.2	0.2	0.616	0.996	0.6161	23.4
39.0	39.1	0.4	0.713	0.990	0.6100	22.5
39.0	64.5	0.4	0.570	0.990	0.6100	22.8
55.0	115.0	0.1	0.442	0.993	0.6161	18.9
55.0	115.0	0.1	0.447	0.993	0.6161	18.6
70.0	118.6	0.1	0.479	0.995	0.6161	16.5
85.0	118.6	0.1	0.500	0.995	0.6161	15.5
100.0	118.6	0.1	0.520	0.995	0.6161	14.7
110.0	71.0	1.0	0.684	0.985	0.6120	13.8
113.0	118.6	0.1	0.542	0.995	0.6161	13.7
130.0	72.8	1.7	0.699	0.987	0.6120	12.9
130.0	44.5	0.8	0.806	0.994	0.6120	12.7

As the experimentally determined potential law constant; K, is much larger than K_p obtained by consideration of the polarizability of the hydrogen molecule alone, other and perhaps valence forces are involved.

In the range from 24 to 135 volts ($r_a=1.74$ to 1.5A), $Q=1771$.

$$V=-\frac{9.58\times10^{-14}}{r^{1.74}} \tag{23}$$

using Eq. (13) but

$$V=-\frac{8.68\times10^{-14}}{r^{1.74}} \tag{24}$$

when K is found using the correction factor f. In Fig. 4 these potential functions are plotted and compared with the curve calculated on the basis of polarization interaction. If the equilibrium distance of the third hydrogen atom in H_3^+ is taken as 1.5A from a line joining the centers of the other two atoms, and an interaction based upon these potential laws is used, the interaction energy is calculated to be 3.01 electron volts. If Eq. (20) alone is used, 4.02 electron volts is obtained. This is to be compared with 3.5 ev given previously.[1]

The measurements taken with H_3^+ are given

in Table II and in Fig. 2. The logarithmic plot in Fig. 3, shows very little curvature; and from it, $\log Q=2.020$ and $n=4.60$, if it is assumed to be a straight line between 5.4 and 130 volts ($r_a=2.12$ to 1.07A). $K_a=1.86\times10^{-36}$, $f=0.616$, and $K=1.145\times10^{-36}$.

Between 10.5 and 28 volts ($r_a=1.85$ to 1.48A) the data correspond closely to a straight line of slope, $n=4$ and $\log Q=2.105$; $K_a=9.3\times10^{-32}$ from Eq. (13) and $f=0.643$ or

$$V=-\frac{5.98\times10^{-32}}{r^4}. \tag{25}$$

This is seen to be very nearly the potential law as evaluated on the basis of polarizability (22).

THE JOURNAL OF CHEMICAL PHYSICS VOLUME 11, NUMBER 7 JULY, 1943

The Low Velocity Scattering of H_2^+ in Hydrogen. The Determination of Neutralization

J. H. SIMONS, C. M. FONTANA, H. T. FRANCIS, AND L. G. UNGER
School of Chemistry and Physics, The Pennsylvania State College, State College, Pennsylvania

(Received February 2, 1943)

Measurements of the effective cross-sectional area for neutralization have been made for H_2^+ in hydrogen over a velocity range of 4 to 30 volts. As this is an electron transfer phenomenon, its measurement is of some theoretical interest. The technique of the method of measurement is discussed and possible experimental uses for it are suggested. The ability to make these measurements has enabled the elastic scattering of H_2^+ in hydrogen to be determined. In the range of 10 to 25 volts ($r_a=2.14$ to 1.70A), the potential law found is $V=-\frac{10.0\times10^{-32}}{r^4}$. As the constant, K, in this equation is considerably greater than an interaction based upon the polarizability of the hydrogen molecule, other forces such as those causing valence bonds must come into play in addition. Above 25 volts ($r_a<1.70$A) the potential law becomes $V=-\frac{6.96\times10^{-24}}{r^3}$.

IN our preliminary work on the scattering of hydrogen ions in hydrogen[1] consistent results were not obtained with H_2^+ because of the occurrence of neutralization or collision of the second kind. This is the transfer of an electron from the gas molecule to the positive ion leaving the latter electrically neutral and making an ion of the gas molecule. Of course, this would be expected to occur to an appreciable extent in only those cases where the ionization potential of the molecule were equal to or below the electron affinity of the positive ion. As H_2^+ and H_2 are identical except for one electron, neutralization could be expected. With the two particles stationary and at close distance the probability of the electron being on one of them is $\frac{1}{2}$. This phenomenon has been previously discussed and investigated.[2] The scattering apparatus[3] was designed to make quantitative measurements of the effective cross-sectional area for neutralization as a function of the velocity of the moving ion. With the ability to separate the neutralization and elastic scattering the measurement of the interaction of H_2^+ with H_2 has become possible and is herein reported.

THE MEASUREMENT OF NEUTRALIZATION

A sketch of the measuring tube is shown in Fig. 1. Below the collimating devices is the scattering cylinder, *SC*, which has a separately insulated cover, *SCL*. Below this is the collecting

[1] A. S. Russell, C. M. Fontana, and J. H. Simons, J. Chem. Phys. **9**, 381 (1941).

[2] T. R. Hogness and E. G. Lunn, Phys. Rev. **28**, 849A (1926); G. P. Harnwell, ibid. **29**, 683, and 830 (1927); H. D. Smyth and E. C. G. Stueckelberg, ibid. **32**, 779 (1928).

[3] J. H. Simons, H. T. Francis, C. M. Fontana, and S. R. Jackson, Rev. Sci. Inst. **13**, 419 (1942).

cylinder, *CC*. Each of these parts is separately connected to the electrical measuring devices. A small decelerating potential on *SCL*, negative with respect to *SC*, will attract and collect slow-moving ions. The ions formed by neutralization have thermal velocities. As elastically scattered ions will in general be scattered less than 90° and will have relatively large velocities compared to thermal velocities; this small potential difference will affect them but slightly, whereas it will sweep the ions formed by neutralization upward to the *SCL*.

The following analysis will assume that all ions undergoing elastic scattering are collected on *SC* and that all slow moving ions formed by neutralization are collected on *SCL*. There are several defects in this assumption, but they tend to counterbalance one another. An ion formed by neutralization will have initially random motion and will in general be counted on the *SCL* regardless of further acts of collision. On the other hand, an ion that has suffered an elastic collision may subsequently suffer either another elastic collision or be neutralized. A second collision will only infrequently change the measurement, as the probability is small of a second elastic collision deflecting the ion either through the exit hole or up to the *SCL*. If, however, the scattered ion undergoes neutralization, it has a good chance of being counted as neutralized instead of scattered. An effect which counterbalances this error is that the neutralization may take place low in the cylinder. In this case the small negative potential on the lid will not be sufficient to collect the ions in order to be counted as neutralized. Scattered ions that become neutralized near the cylinder wall will still be counted as scattered as the neutralized ion will drift to the wall. As the probability of a second collision act is small under the conditions of operation and as the various secondary effects tend to be in opposite directions, the primary assumptions are probably reasonable.

There is an additional uncertainty in the measurements when the *SCL* retarding potential is used. The velocity of the ion beam changes slightly in passing through the scattering cylinder due to the retarding field and, consequently, undergoes a small amount of focusing. The measurements obtained indicate that these uncertainties cannot contribute greatly. They will be relatively greater in the low velocity end of the data. A system of grids in the scattering cylinder may overcome some of these uncertainties, but until more knowledge is obtained in this work, the complications introduced both experimentally and theoretically by this added refinement would greatly increase the difficulties.

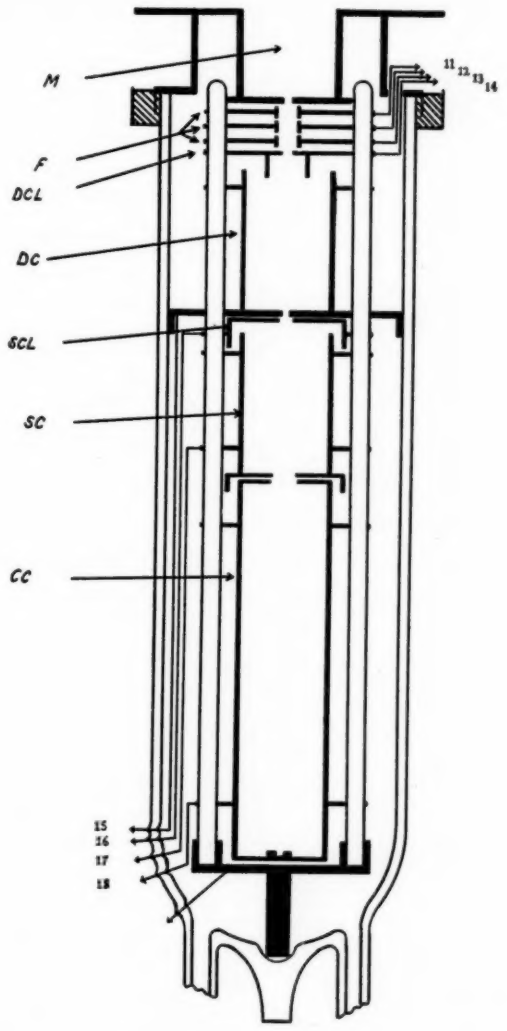

FIG. 1. The measuring tube.

The magnitude of the negative potential to be applied is determined by measuring the *SCL* ion current for different values of retarding potential. For the first few volts the increase in current is appreciable, but above four or five volts it becomes relatively small. A four- or five-

TABLE I. The neutralization and scattering of H_2^+ in H_2.

W in Volts	$P\times10^4$ mm	R_T	R_T°	R_S	R_S°	F	$\frac{R_T}{R_T^\circ}$	$\frac{R_S}{R_S^\circ}\left[1-(1-R_S^\circ)\frac{\alpha_N}{\alpha_S}\right]$		α_T	α_S	α_N
70	55.15	0.432	0.997	0.645	0.997	0.613	0.433	0.647	0.996	40.6	16.8	23.8
50	55.15	0.393	0.998	0.597	0.998	0.613	0.393	0.598	0.997	45.1	19.7	25.4
35	26.65	0.601	0.998	0.753	0.998	0.612	0.602	0.754	0.998	51.0	25.1	25.9
25	26.65	0.553	1.000	0.700	0.994	0.612	0.553	0.704	0.995	59.5	31.6	27.9
15	26.75	0.490	0.993	0.613	0.989	0.612	0.494	0.619	0.992	70.6	41.9	28.7
9.8	26.75	0.436	0.992	0.551	0.984	0.612	0.439	0.560	0.990	82.4	50.1	32.3
5.5	26.75	0.381	0.990	0.480	0.992	0.612	0.384	0.484	0.996	95.8	63.4	32.4
3.3	26.75	0.331	0.925	0.419	0.951	0.612	0.357	0.452	0.980	103.3	68.2	35.1

Note. As a retarding potential of 5 volts was used the incoming ions are 5 volts faster than W. $P_0=0.20\times10^{-4}$ mm throughout.

volt retarding potential is therefore used in most measurements.

There are several ratios of current which can be measured. If the currents to the several parts are represented as I_{scL}, I_{sc} and I_{cc} when the retarding potential is not in use and I'_{scL}, I'_{sc} and I'_{cc} when it is in use, we can define the ratios as

$$R_T=\frac{I_{cc}}{I_{scL}+I_{sc}+I_{cc}},\quad R_S=\frac{I'_{cc}}{I'_{sc}+I'_{cc}},$$

and

$$R_N=\frac{I'_{scL}}{I'_{scL}+I'_{sc}+I'_{cc}}. \tag{1}$$

If, because of the inability to obtain a zero pressure and to align the apparatus perfectly, a low pressure is used for control purposes, we can define the ratios obtained at this low pressure as R_T^0 and R_S^0. From the measurements of R_T, R_T^0, R_S and R_S^0 the effective cross-sectional area due to elastic scattering, α_S, and neutralization, α_N, can be evaluated. R_S is used rather than R_N because in the measurement of R_N it is necessary to measure currents from elements at different potentials, whereas for R_S they are at the same potential. The use of R_N does, however, give an independent check to the measurements.

$$\alpha_T=\alpha_S+\alpha_N. \tag{2}$$

$$dI_T=IP\alpha_T dx. \tag{3}$$

As $I=I_0-I_T$ when I_T is the loss in intensity of the ion beam caused by both elastic scattering and neutralization up to point x,

$$\alpha_T=\frac{2.303}{l(P-P_0)}\log\frac{R_T^0}{R_T}.^4 \tag{4}$$

Also

$$dI_S=IP\alpha_S dx,\quad\text{and}\quad dI_N=IP\alpha_N dx. \tag{5}$$

$$dI_S/dI_T=\alpha_S/\alpha_T,\quad\text{and}\quad dI_N/dI_T=\alpha_N/\alpha_T.$$

$$\alpha_T I_S=\alpha_S I_T,\quad\text{and}\quad \alpha_T I_N=\alpha_N I_T.$$

$$\alpha_S=\alpha_T\frac{I_S}{I_T}=\alpha_T\frac{(I'_{sc}+I'_{cc}-I'_{cc})/I'_{cc}}{(I'_0-I'_{cc})/I'_{cc}}. \tag{6}$$

For $I_0'=I_0$ and $I'_{cc}=I_{cc}$, because the inclusion of the retarding potential changes neither the intensity of the entering beam nor the intensity of the undeflected portion of it

$$\alpha_S=\alpha_T\frac{(1/R_S)-1}{(1/R_T)-1}. \tag{7}$$

Similarly,

$$\alpha_N=\alpha_T R_N/(1-R_T). \tag{8}$$

To correct for the fact that P_0 is not zero and the apparatus is not perfect, a small correction term can be obtained. When this is included a corrected value is given by

$$\alpha_S=\alpha_T\frac{(R_S^0/R_S)-1}{(R_T^0/R_T)-1}\left[1-(1-R_S^0)\frac{\alpha_N}{\alpha_S}\right]. \tag{9}$$

The term $[1-(1-R_S^0)(\alpha_N/\alpha_S)]$ is obtained using preliminary values of α_N and α_S from Eqs. (2), (7), and (8).

[4] Preceding paper, J. H. Simons, C. M. Fontana, E. E. Muschlitz, Jr., and S. R. Jackson, "The low velocity scattering of H^+ and H_3^+ in hydrogen."

RESULTS

The results of the experimental measurements are shown in Table I and Fig. 2.

The elastic scattering of H_2^+ in H_2 corresponds within experimental error to an inverse fourth-power potential law in the range 10 to 25 volts ($r_a=2.14$ to 1.70A). Here $Q=159$, $K_a=14.4\times10^{-32}$, and $f=0.696$.[5]

$$V=-\frac{10.0\times10^{-32}}{r^4}. \tag{10}$$

Below 10 volts ($r_a>2.14$A) the potential falls off more rapidly than Eq. (10). Above 25 volts ($r_a<1.70$A) the law becomes an inverse third-power potential law.

$$K_a=9.2\times10^{-24}, \quad f=0.757,$$

and

$$V=-\frac{6.96\times10^{-24}}{r^3}. \tag{11}$$

It is also of interest to note that in the plot of α_S *vs.* W the curve for H_2^+ is located between the curves for H^+ and H_3^+ and intersects at an approximately common point.

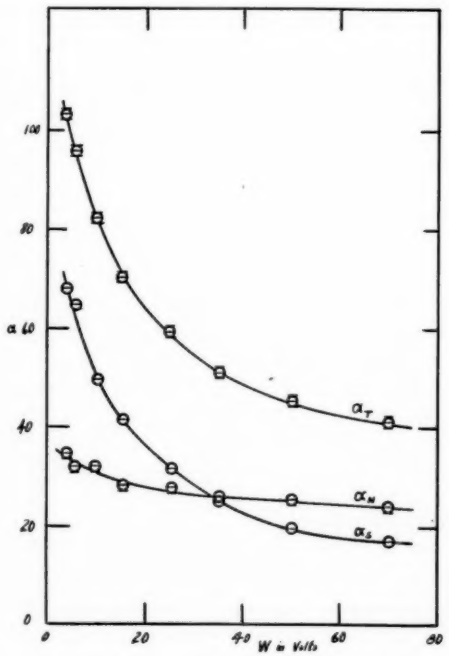

FIG. 2. The effective cross-sectional area of H_2 for scattering and neutralizing H_2^+.

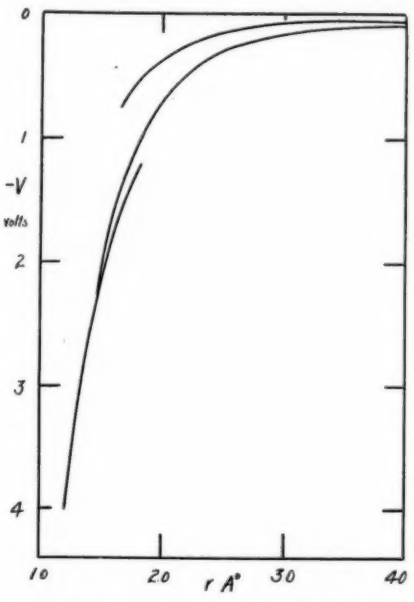

FIG. 3. Potential energy of H_2^+ and H_2. The upper curve represents the potential calculated on the basis of the interaction of the charge on the ion with the induced dipole of the molecule.

The potential laws for H_2^+ in H_2 are plotted in Fig. 3. A comparison with the potential law calculated on the basis of the polarizability of the hydrogen molecule shows that this effect alone is not sufficient.

The effective cross section for neutralization, α_N, shows only a small deviation with velocity. On the assumption of equal probability of finding the extra electron on either particle after collision involving nearer approach than a constant distance, r_N, the expression for the increment of neutralized current should be modified by the probability factor $\frac{1}{2}$.

$$dI_N=\tfrac{1}{2}INP\pi r_N^2dx. \tag{12}$$

Combining with Eq. (5)

$$r_N=(2\alpha_N/\pi N)^{\frac{1}{2}}. \tag{13}$$

Taking $\alpha_N=30$ from the experimental results $r_N=2.3$A. This is a reasonable range for the electron distribution about a hydrogen molecule.

The curve for α_N apparently approaches a finite value as W approaches zero. This is reasonable as there is no change of energy content in the process and with the ions moving

[5] J. H. Simons, E. E. Muschlitz, Jr., and L. G. Unger, "The scattering of low velocity hydrogen ions in helium," p. 322, this issue.

infinitely slowly there is an equal chance of the charge being on either particle.

POSSIBLE USES

Besides the use of measurements of the effective cross-sectional area for neutralization, α_N, for theoretical purposes, there are experimental uses for the results of these experiments. (The neutralization is in a sense the probability of electron transfer and as such may have theoretical implications.) The ions that are neutralized in the scattering cylinder become a stream of fast moving neutral particles with a velocity range that can be held within close limits. This would furnish a good source for molecular beam studies where a selection of a narrow velocity range is one of the greatest difficulties. This has been used by Amdur and Pearlman[6] for beams of atomic hydrogen by the passage of the ions of the hydrogen arc through hydrogen gas. It would appear from our results that no hydrogen atoms are formed from the reaction of any of the ionic species of hydrogen with hydrogen molecules. However, the neutralization of protons by water vapor[7] would result in hydrogen atoms. This may explain why it is general practice to have water vapor present in the electrodeless discharge tube used to form beams of hydrogen atoms. The hydrogen atoms are probably formed by the neutralization of protons by water vapor.

Another possible use for the neutralization technique would be the production of thermal ions. Perhaps the specificity of this reaction would enable pure streams of desired ions to be formed. These ions with thermal velocities may have other uses such as in studies of equilibria.

[6] I. Amdur and H. Pearlman, J. Chem. Phys. **8**, 7 (1940).

[7] See following paper, J. H. Simons, H. T. Francis, E. E. Muschlitz, Jr., and G. C. Fryburg, "The scattering of low velocity hydrogen ions in water vapor."

THE JOURNAL OF CHEMICAL PHYSICS VOLUME 11, NUMBER 7 JULY, 1943

The Scattering of Low Velocity Hydrogen Ions in Water Vapor

J. H. SIMONS, H. T. FRANCIS, E. E. MUSCHLITZ, JR., AND G. C. FRYBURG
School of Chemistry and Physics, The Pennsylvania State College, State College, Pennsylvania

(Received February 2, 1943)

The elastic scattering of H^+, H_2^+, and H_3^+ in water vapor has been measured in the velocity range 2 to 130 volts. For H^+ the potential law for 3 to 15 volts ($r_a = 2.74$ to 1.77A) is $V = -\frac{6.33\times10^{-32}}{r^4}$. Assuming an equilibrium distance of 1.013A the proton affinity of H_2O is calculated to be 6.5 electron volts. Above 15 volts ($r_a < 1.77$A) the coefficient of r becomes very large (about 20). For H_2^+ in H_2O between 3 and 20 volts ($r_a = 3.14$ to 2.33A) $V = -\frac{193\times10^{-56}}{r^7}$. Above 20 volts the coefficient of r increases to a much larger value (about 13). H_3^+ in H_2O shows a potential law $V = -\frac{8.7\times10^{-16}}{r^2}$ between 5 and 20 volts ($r_a = 4.27$ to 2.33A). This is about what would be expected on the basis of the interaction of a dipole and a charge. Between 20 and 30 volts the coefficient of r becomes 3 and from 30 to 60 volts it is much larger (about 8). Neutralization is experienced with both H^+ and H_2^+ in H_2O but not with H_3^+. These neutralization cross sections are reported as a function of velocity. A design is given of a Knudsen gauge found satisfactory for the measurement of the pressure of water vapor. A new technique is described which was found necessary for the removal of insulating films on the metallic surfaces. These films are apparently carbonaceous and formed by the action of the ion beam on traces of organic compounds in the vapor. The technique used is an electric discharge in oxygen.

PREVIOUS attempts[1] to measure the scattering of low velocity hydrogen ions in water vapor were not satisfactory for two reasons. The ability to measure the neutralization phenomenon had not been developed and the measurement of pressure was unsatisfactory. By using

[1] A. S. Russell, C. M. Fontana, and J. H. Simons, J. Chem. Phys. **9**, 381 (1941).

our new apparatus[2] the neutralization was found measurable.[3] A Knudsen gauge was constructed and used for the pressure measurements. Reproducible results now have been obtained for both elastic scattering and neutralization of all three hydrogen ions in water vapor and are herein reported.

APPARATUS

The equipment used was essentially that previously described[2] with the exception of the Knudsen gauge. This gauge is reported[4] to be capable of measuring pressures of either condensable or non-condensable gases and without dependence upon the molecular weight or other specific property. As a somewhat different design of the gauge was constructed and used, it is herein described. A diagram is shown in Fig. 1. The glass envelope, A, was made from the neck of a 12-liter round-bottom flask. The flanged end was ground smooth and fitted with a rubber gasket, B, and a brass ring, C. Brass machine screws, D, permitted drawing the envelope securely up against the circular brass plate, E, which served as a support for the working parts of the gauge. The seal between the ground glass flange and the brass plate was effected by coating the rubber gasket with "plicene," drawing the assembly tight, warming until the plicene was molten and tightening further. Bracket, F, secured brass bar, G. This carried a small, flat, insulated frame, H, on which was wound about 3 feet of nichrome ribbon, I. One end of the ribbon made electrical contact with the bar at J. The other end contacted the insulated connection, K. A six-volt battery supplied the current (about 0.2 amp.) for the "heater strip," which had a resistance of 4.8 ohms. The brass screw, L, supported the aluminum foil, M, of dimensions $6'' \times \frac{1}{4}'' \times 0.00025''$. The deflection of the foil was observed with a microscope equipped with an ocular scale such that 22 scale divisions equalled 1-mm deflection. This gauge was calibrated against a McLeod gauge in the region, 5 to 40×10^{-4} mm. The precision of the measurements is difficult to estimate but judging from the calibration curve it is better than ± 5 percent.

PROCEDURE

Water was supplied from a sample of well degassed liquid held at 0°C. It entered the apparatus through a series of capillary leaks.

As the establishment of pressure equilibrium between the water vapor and glass and other parts of the apparatus required considerable time due to slow adsorption and desorption, a different technique of measurement was employed from that used previously for non-condensable gases. For hydrogen gas where pressure equilibrium was quickly established, it was convenient to change the pressure while keeping the electrical controls constant and so obtain scattering measurements for one kind of ion at the same velocities but at different pressures. With water it was necessary to keep the pressure constant and change the electrical controls. The technique used follows:

After pressure equilibrium was established, the ion source was put into operation and the various focusing elements before and after the magnet chamber as well as the magnet current itself were adjusted to give maximum beam current of the desired ion species to the collecting cylinder of the measuring tube. The potentials applied to the various elements in the measuring tube were

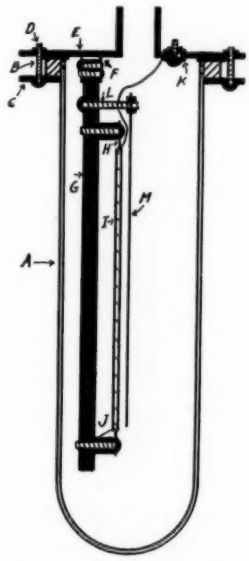

FIG. 1. Knudsen gauge.

[2] J. H. Simons, H. T. Francis, C. M. Fontana, and S. R. Jackson, Rev. Sci. Inst. **13**, 419 (1942).
[3] Preceding paper. J. H. Simons, C. M. Fontana, H. T. Francis, and L. G. Unger, "The low velocity scattering of H_2^+ in hydrogen. The determination of neutralization."
[4] A. L. Hughes, Rev. Sci. Inst. **8**, 409 (1937).

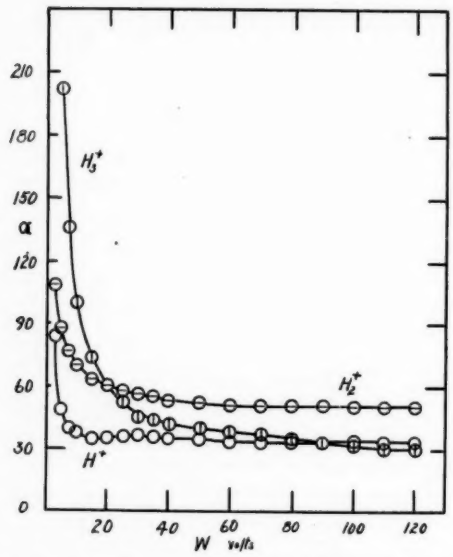

FIG. 2. The effective cross-sectional area of H_2O for scattering H^+, H_2^+, and H_3^+.

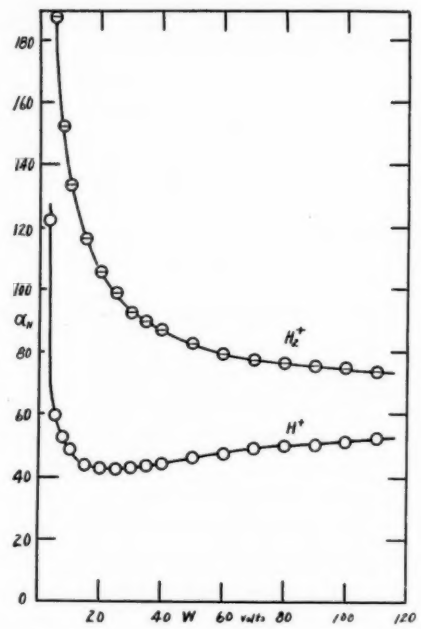

FIG. 3. The effective cross-sectional area of H_2O for neutralizing H^+ and H_2^+.

adjusted to the same value, namely cathode potential. This arrangement caused the ions to have a velocity of about 130 volts—the maximum value used in this work. The amplifier used to measure the small beam currents in the measuring tube was put into operation, and the currents reaching *CC* alone and the total reaching *CC*, *SC*, and *SCL* were measured. This gave the ratio, $R_T=I_{CC}/(I_{CC}+I_{SC}+I_{SCL})$. This was reproducible to better than one percent. The velocity of the ions in the beam was then determined by measuring the decelerating potential necessary to stop the beam.

These measurements were then repeated at lower velocities. The total number of velocities at which ratios were taken was usually about fifteen extending from 130 to about 2 volts. A plot of R_T against W (velocity in volts) was made. This was repeated for the two other ion species. The potentials to the elements of the measuring tube were now readjusted. *DCL*, *DC*, and *SCL* were at the same potential but this was four volts more negative than the potential to *SC* and *CC*. The values of the currents to *SCL*, *SC*, and *CC* were separately measured. $R_S=I'_{CC}/(I'_{SC}+I'_{CC})$ and is thus determined. Its reproduceability was better than one percent. The ion velocity is determined and the measurements repeated at lower velocities. A plot of R_S against W was prepared. After a set of measurements of this kind was made at one pressure, they were repeated at another pressure.

The data are now in the form of curves of R_T and R_S at several pressures. From values of R_T at even voltages and different pressures α_T is calculated from

$$\alpha_T=\frac{F}{P_2-P_1}\log\frac{R_1}{R_2}. \qquad (1)$$

TABLE I. The scattering of hydrogen ions in water.

W Volts	H^+ α_T	H^+ α_S	H^+ α_N	H_2^+ α_T	H_2^+ α_S	H_2^+ α_N	H_3^+ $\alpha_T=\alpha_S$
3	206.3	83.5	122.8	339	109.3	229.7	278.0
5	108.0	48.5	59.5	277	89.6	187.4	202.7
7.5	93.1	40.2	52.9	230	77.5	152.5	136.1
10	86.6	38.0	48.6	204	70.0	134.0	100.6
15	78.1	34.9	43.2	180	63.6	116.4	73.1
20	78.2	35.6	42.6	166	60.0	106.0	60.0
25	78.4	35.9	42.5	157	58.0	99.0	51.5
30	79.0	36.1	42.9	149	56.1	92.9	45.7
35	79.4	35.5	43.9	145	54.9	90.1	44.0
40	79.8	35.6	44.2	141	53.5	87.5	42.5
50	80.5	34.4	46.2	136	52.6	83.4	40.3
60	81.1	33.4	47.7	131	51.5	79.5	38.6
70	82.6	33.3	49.3	129	51.2	77.9	37.3
80	83.3	33.3	50.0	127	50.3	76.7	35.4
90	83.9	33.7	50.2	126	50.6	75.4	33.8
100	85.0	33.7	51.3	125	50.1	74.9	32.2
110	86.0	33.6	52.4	124	50.7	73.3	31.0
120	87.0	33.6	53.4	123	50.3	72.7	30.1
130	87.9	33.7	54.2	122	50.6	71.4	29.4

From the values of R_S and R_T at one pressure and the same voltage α_S is calculated.

$$\alpha_S=\alpha_T\frac{(1/R_S)-1}{(1/R_T)-1}. \qquad (2)$$

It is then calculated at the same voltage but at another pressure and the values averaged. α_N is obtained by difference for $\alpha_T=\alpha_S+\alpha_N$.

Removal of Carbonaceous Films

After the apparatus had been in use for some time difficulties were encountered in unsteady currents. We had previously encountered unsteady currents and had corrected them by sparking the apparatus while it contained a significant pressure of hydrogen. We had judged the trouble to be caused by insulating oxide films on the metallic surfaces which were reduced by the atomic hydrogen treatment. The present difficulty was of the same nature as the former but was not eliminated by the reduction procedure. Colored films were observed on the metallic surfaces where the ion beam impinged. Stewart[5] discussed a similar phenomenon and decided that these insulating films were caused by carbon compounds that were formed by the action of the ion or electron bombardment on residual organic vapor present, probably from the grease on stopcocks. These films are not soluble in ordinary solvents.

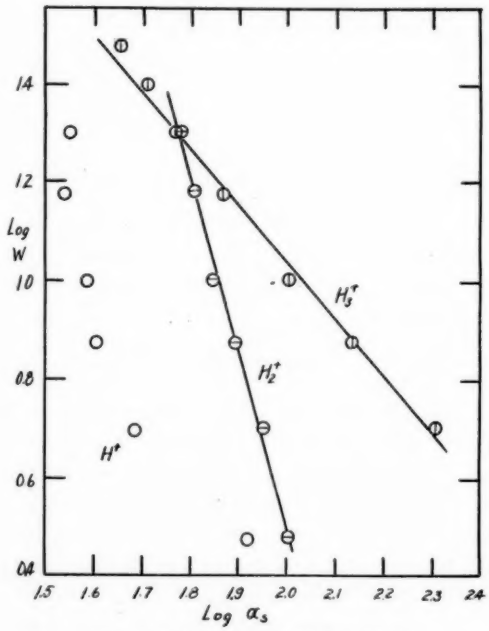

FIG. 4. H^+, H_2^+, and H_3^+ in H_2O.

[5] R. L. Stewart, Phys. Rev. **45**, 488 (1934).

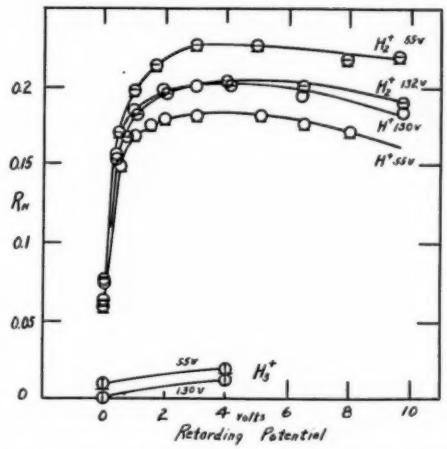

FIG. 5. The separation of ions formed by neutralization.

The procedure adopted was similar to the reduction technique except that it was an oxidation technique. With about two mm of oxygen pressure in the apparatus the sparking procedure was carried out. The purpose of this was to burn the film. The oxygen was now removed, hydrogen added, and the apparatus resparked to complete the procedure. This enabled the apparatus to be used for another considerable period of time (six months) before the oxidation procedure was again necessary.

RESULTS

H^+ in Water Vapor

The effective cross-sectional areas for H^+ in H_2O are given in Table I and shown in Figs. 2 and 3. As described above, the ratios were initially plotted and a smooth curve drawn through them. The curves herein given do not, therefore, show the deviation of the experimental points; but the reproduceability of both R_S and R_T was within one percent and the deviations of the points from a smooth curve were approximately the same as shown in the previous work[3] using hydrogen gas.

The logarithmic plot for the elastic scattering, α_S, in Fig. 4 indicates a potential law that cannot be easily represented in a simple form. However, an approximate fit from 3 to 15 volts ($r_a=2.74$

to 1.77A) is found with $n=4$.

$$K_a=8.33\times10^{-32},$$

and as $f=0.82$,[6]

$$V=-\frac{6.33\times10^{-32}}{r^4}. \quad (3)$$

Assuming that the equilibrium distance in the H_3O^+ ion is the same as the O−H distance in water (1.013A) and that the above potential law holds down to this distance, a value for the proton affinity of water is 6.5 ev, or 150 kcal. per mole. The heat of hydration of H^+ was calculated by Sherman[7] to be 182 kcal. per mole. It is given by Goubreau[8] as 260 kcal. per mole. The distance assumed above is probably too large as the H_3O^+ ion is very stable and the distances may be less than in water. A shorter distance would give a larger value of proton affinity. In view of the assumptions involved and the change of potential law with distance shown in Fig. 4, this value for the proton affinity is only tentative.

Above 15 volts (r_a less than 1.77A) n becomes very large (about 20).

H_2^+ in Water Vapor

The cross-sectional areas for H_2^+ in H_2O are shown in Table I and in Figs. 2 and 3. Between 3 and 20 volts ($r_a=3.14$ to 2.33A), $n=7$.

$$K_a \text{ is } 260\times10^{-56},$$

and $f=0.74$ from a long extrapolation of Fig. 5, reference (6).

$$V=-\frac{193\times10^{-56}}{r^7}. \quad (4)$$

Above 20 volts (r_a less than 2.33A) the value of n is much greater (about 13).

H_3^+ in Water Vapor

Neutralization was not experienced with H_3^+ in H_2O. The total cross-sectional area is, therefore, the elastic scattering area. It is shown in Table I and in Figs. 2 and 4. Between 5 and 20 volts ($r_a=4.27$ to 2.33A), $n=2$ and $K_a=9.6\times10^{-16}$. As $f=0.908$,

$$V=-\frac{8.7\times10^{-16}}{r^2}. \quad (5)$$

At higher voltages ($W=20$ to 30 volts) n becomes about 3, and from 30 to 60 volts it becomes higher (about 8).

As the water molecule is a permanent dipole, an interaction of this dipole with the charge on an ion should follow an inverse square potential law.

$$V=-\mu ze/r^2, \quad (6)$$

where μ is the dipole moment which for water is 1.87×10^{-18} e.s.u. This gives

$$V=-\frac{5.60\times10^{-16}}{r^2}. \quad (7)$$

It is interesting to note that the experimentally determined interaction is approximately that given by Eq. (7).

In Fig. 5 is shown a plot of preliminary measurements made to determine a suitable retarding potential to be used in the measurement of neutralization. This is given in terms of $R_N=I'_{scL}/(I'_{scL}+I'_{sc}+I'_{cc})$. As four volts seem to give a maximum current to the scattering cylinder lid, it was chosen as the suitable value. A small ratio at zero retardation potential is to be expected because of thermal diffusion of the slow ions. The decrease in R_N above four volts is probably due to the focusing or defocusing effect on the beam of large values of this voltage. The values of R_N for H_3^+ at two voltages are also given. These show that there is no significant neutralization for H_3^+.

DISCUSSION

It can be pointed out that in scattering measurements of this kind the force field must be assumed to be spherically symmetrical. Either the interacting particles rotate to present the same side to each other as they pass (as a dipole would be expected to rotate to a passing ion), or the force calculated is the spherical average of that which different directions would produce. If the force is greatly different in different directions, rotation would be expected.

[6] Following paper. J. H. Simons, E. E. Muschlitz, Jr., and L. G. Unger, "The scattering of low velocity hydrogen ions in helium."
[7] J. Sherman, Chem. Rev. **11**, 93 (1932).
[8] J. Goubreau, Zeits. f. physik. Chemie **B34**, 432 (1936).

The distance of closest approach, r_a, as shown in this work is, of course, an average distance for all ions scattered at that velocity. A mixture of potential laws (attractive and repulsive) may be expected to be operating at any r_a.

Measurements of this kind cannot distinguish between attractive and repulsive forces as scattering could be experienced by either. The high values of n for close distances of approach may be related to repulsion.

In obtaining numerical values for the energy of combination, for example, proton affinities, two assumptions are made. First an equilibrium distance must be assumed, and a large uncertainty is thus introduced. It is also assumed that this classical law can be used down to such close distances. This, of course, is only a first approximation; but as the integration extends from this value to infinity and as the classical law is more and more nearly correct as the distance becomes larger, this assumption is certainly completely justified in view of the uncertainty of the equilibrium distance.

The curves for the neutralization cross section, α_N, plotted against voltage, W, show some interesting differences. For H^+ and H_2^+ in H_2O the curves (values of α_N) rise steeply as W approaches zero, whereas for H_2^+ in H_2 it does not.[3] This is reasonable for there is an energy release in the reactions,

$$H^+ + H_2O \rightarrow H_2O^+ + H$$

and

$$H_2^+ + H_2O \rightarrow H_2O^+ + H_2,$$

whereas in the reaction

$$H_2^+ + H_2 \rightarrow H_2 + H_2^+$$

there is no over-all energy change. This would cause a much greater probability of reaction at low velocities in water. The two neutralization curves for H^+ and H_2^+ in water show an appreciable difference. The former has a definite minimum at about 20 volts. The minimum can be rationalized on the following basis. As the velocity of the ion passing a molecule in which neutralization can take place increases, there are two effects that may influence the probability of the interaction. First, the time of passing through a specified region of collision decreases as the velocity increases; and second, the average distance of approach of the two centers decreases as the velocity increases. The first should decrease the probability of interaction and the second increase it. The summation of these two effects could give a minimum under suitable conditions.

THE JOURNAL OF CHEMICAL PHYSICS VOLUME 11, NUMBER 7 JULY, 1943

The Scattering of Low Velocity Hydrogen Ions in Helium

J. H. SIMONS, E. E. MUSCHLITZ, JR., AND L. G. UNGER
School of Chemistry and Physics, The Pennsylvania State College, State College, Pennsylvania

(Received February 2, 1943)

The low velocity scattering of H^+, H_2^+ and H_3^+ in helium was measured. No neutralization was experienced and the potential laws were evaluated. For H^+ in the range 3 to 130 volts (r_a=2.66 to 0.55A), $V=-\frac{1.36\times10^{-18}}{r^{2.27}}$. For H_2^+ in the range 4 to 50 volts (r_a=1.67 to 0.87A), $V=-\frac{1.47\times10^{-32}}{r^4}$. In the range 50 to 120 volts (r_a=0.87 to 0.66A), $V=-\frac{1.31\times10^{-32}}{r^4}$. For H_3^+ in the range 1.5 to 14 volts (r_a=2.22 to 1.59A), $V=-\frac{3.9\times10^{-53}}{r^{6.68}}$. In the range 14 to 65 volts (r_a=1.59 to 1.12A), $V=-\frac{1.06\times10^{-24}}{r^{4.46}}$. In the range 65 to 130 volts (r_a=1.12 to 0.89A), $V=-\frac{4.83\times10^{-24}}{r^{3.01}}$. The interaction of H^+ in He shows the effect of the chemical combination to form HeH^+. Assuming an equilibrium distance of 0.8A, the interaction energy is 3.27 ev. H_2^+ in He follows the law expected on the basis of the interaction of the charge on an ion with a polarizable molecule. The interaction of H_3^+ with He is more complex. An exact analytical treatment of the scattering problem shows that n, calculated from the experimental data by the previously used general approximate method, is correct. An exact numerical solution is given for the case $n=4$ and several values of the mass ratio of ion to molecule and values of f_c obtained, where $f_cK_a=K_e$. A less laborious method of calculating f, involving a simplifying assumption, is used; and it is shown that $f_c=f$ well within the precision of the experiments. A similar method is used to calculate f for the same mass ratios and $n=0$, 1, and 2. A family of curves is obtained from which values of f can be interpolated for other values of n and mass ratio.

OUR previous low velocity scattering measurements were all made in diatomic and polyatomic gases. It was hoped that the scattering in a monatomic gas would be of theoretical interest and perhaps aid in the theoretical interpretation of our other work. Consequently, the present measurements were made using helium. The results for elastic scattering of H^+, H_2^+, and H_3^+ are herein reported. Neutralization was neither expected nor found.

In a preceding paper[1] a general but approximate analytical treatment of the scattering problem was given and this was used in the next two papers.[2] It is possible to make an exact analysis of this problem for certain values of m_1/m_2 and n, where m_1 and m_2 are the masses of the ion and molecule, respectively, and n is defined in Eq. (1). This has been done for $n=4$ and a number of values of m_1/m_2. It can be seen from this analysis that the value of n obtained by an exact treatment will be identical with the value obtained using the simpler equations from the approximate treatment. The constant K in the equation,

$$V=-K/r^n, \tag{1}$$

is given by a different function of the experimental data and the apparatus dimensions in the approximate and exact analyses, and has a somewhat different numerical value. This method is laborious and an easier one is used in which the assumption of a small angle of scattering is made. A comparison of the numerical values obtained by the two methods in the case $n=4$ (Table IV) shows that they agree within the experimental precision of the apparatus used. For a mass ratio of zero the two methods give the same result. The less laborious method is then used for $n=0$, 1, and 2 for several values of mass ratio; and values of the constant, K, are calculated. These are compared with K_a, the value of the constant calculated on the basis of the general approximate analysis; and a multiplying factor, f, is obtained. (Table IV.)

$$K=fK_a. \tag{2}$$

A family of curves is plotted in Fig. 5 using the values of f for different values of n and the mass ratio. These curves are then used for interpola-

[1] J. H. Simons, C. M. Fontana, E. E. Muschlitz, Jr., and S. R. Jackson, "The low velocity scattering of H^+ and H_3^+ in hydrogen."

[2] J. H. Simons, C. M. Fontana, H. T. Francis, and L. G. Unger, "The low velocity scattering of H_2^+ in hydrogen. The determination of neutralization." J. H. Simons, H. T. Francis, E. E. Muschlitz, Jr., and G. C. Fryburg, "The scattering of low velocity hydrogen ions in water vapor."

tion for fractional values of n and other mass ratios. If future experiments should require more exact numerical values, it may be possible to use the more rigorous method of evaluating K in a similar way.

The measurements were made in the apparatus previously described.[3] The helium was obtained from the Cryogenic Laboratory of The Pennsylvania State College by the kindness of Dr. J. G. Aston. It was from the United States wells in Texas and stated to be 99.5 percent pure. It was stored over mercury and was passed over activated charcoal at liquid-air temperature in order to remove traces of air before letting it into the scattering apparatus through a capillary leak. The large quantities of liquid air used in all the scattering work were obtained by the kindness of Dr. Aston and the Cryogenic Laboratory.

RESULTS

The results of the scattering of H^+ in He are shown in Table I and Fig. 1, those of H_2^+ in Table II and Fig. 2 and those of H_3^+ in Table III and Fig. 2. The reported values of Ramsauer and co-workers[4] are shown by the crosses in Fig. 1 for comparison. The logarithmic plots are given in Fig. 3.

TABLE I. The scattering of H^+ in helium.

W Volts	$P\times10^4$ mm	$P_0\times10^4$ mm	T °C	R	R_0	α
2.8	36.7	0.3	27.5	0.326	0.965	78.6
3.5	23.8	0.2	31	0.489	0.850	62.5
4.3	35.5	0.2	28	0.494	0.973	50.7
4.9	33.5	0.2	28	0.531	0.976	48.3
5.5	35.0	0.2	28	0.551	0.979	43.6
8.3	71	0.2	30	0.429	0.955	30.0
9.7	72.5	0.2	29.5	0.436	0.935	28.0
10.1	71.2	0.2	29.5	0.475	0.944	25.7
11.0	73.5	0.2	29	0.498	0.952	23.4
17.5	71	0.2	30.5	0.627	0.964	16.19
24	73.5	0.2	29.5	0.698	0.975	12.08
25	72	0.2	32	0.711	0.979	11.92
28	73.5	0.2	32	0.731	0.967	10.20
30.5	74	0.25	26	0.739	0.990	10.41
36	71	0.2	29.5	0.808	0.983	7.32
36.5	75	0.25	26	0.770	0.990	8.83
41.8	74	0.2	32	0.805	0.981	7.16
58.5	87.5	0.2	32.5	0.839	0.981	4.79
69	76.5	0.2	27.5	0.865	0.995	4.83
80	88	0.15	33	0.868	0.983	3.79
96	91.5	0.15	32	0.875	0.981	3.34
117	91	0.1	33	0.880	0.988	3.41
126	93	0.1	32	0.872	0.988	3.61

TABLE II. The scattering of H_2^+ in helium.

W Volts	$P\times10^4$ mm	$P_0\times10^4$ mm	T °C	R	R_0	α
4.0	25.5	0.2	27	0.583	0.787	31.2
4.68	70	0.2	28	0.463	0.960	27.6
6.3	27	0.2	27	0.678	0.863	23.8
9.5	71.5	0.2	29	0.561	0.952	19.64
10.2	26.5	0.3	27	0.746	0.901	19.00
13.0	73.5	0.2	28	0.613	0.952	15.91
14.5	71	0.2	29	0.643	0.963	15.13
21.2	74	0.2	29	0.678	0.973	12.97
25	72	0.2	29	0.710	0.982	11.96
32	69.5	0.2	28.6	0.720	0.960	10.99
39	70.0	0.3	28.6	0.749	0.971	9.86
39	71	0.2	29	0.759	0.980	9.56
48	72	0.2	29	0.782	0.984	8.47
56	67	0.2	27.5	0.821	0.982	7.05
69.3	76	0.2	29	0.821	0.990	6.54
88.5	65	0.2	27	0.856	0.991	5.96
99.3	74	0.2	28	0.854	0.994	5.44
118	58	0.2	27	0.895	1.000	5.04
122	72	0.2	30	0.871	0.994	4.88

TABLE III. The scattering of H_3^+ in helium.

W Volts	$P\times10^4$ mm	$P_0\times10^4$ mm	T °C	R	R_0	α
1.54	65.0	0.2	30	0.212	0.802	54.6
4.3	64.4	0.1	30	0.349	0.927	40.4
7.4	56	0.2	29	0.464	0.944	33.7
8.6	64.8	0.2	31	0.440	0.949	31.7
13.8	55	0.2	29	0.535	0.960	28.2
21.5	53.2	0.2	28	0.612	0.974	23.1
21.7	69	0.2	29	0.505	0.912	22.8
30.8	53.0	0.15	30	0.658	0.977	19.88
31	66.5	0.2	29	0.607	0.992	19.64
39.6	53.0	0.15	30	0.700	0.989	17.39
48.0	53.0	0.15	30	0.720	0.985	15.76
55.7	66.0	0.15	30.5	0.684	0.991	14.98
65.5	65.5	0.1	30	0.704	0.995	14.09
73	66.2	0.1	30	0.724	0.994	12.75
91.5	66.0	0.1	30	0.754	0.995	11.20
105	66.2	0.1	30	0.773	0.996	10.18
119.5	66.8	0.1	30	0.787	0.995	9.35
132	66.8	0.1	30	0.800	0.996	8.74

For H^+ in He a single potential law of the form of Eq. (1) can be used to express the data from 3 to 130 volts ($r_a=2.66$ to 0.55A). Log $Q=2.287$, $n=2.27$, $K_a=1.54\times10^{-18}$ and $f=0.883$.

$$V=-\frac{1.36\times10^{-18}}{r^{2.27}}. \tag{3}$$

This equation is similar to the one[1] obtained from the scattering of H^+ in H_2 in that the value of n is less than 4 and K is relatively large. This may result from similar causes. Both H_3^+ and HeH^+ are known to exist; and a valence attraction is, therefore, contributing to the interaction.

[3] J. H. Simons, H. T. Francis, C. M. Fontana, and S. R. Jackson, Rev. Sci. Inst. **13**, 419 (1942).

[4] C. Ramsauer, R. Kollath, and D. Lilienthal, Ann. d. Physik **8**, 709 (1931); C. Ramsauer and R. Kollath, *ibid.* **16**, 570 (1933).

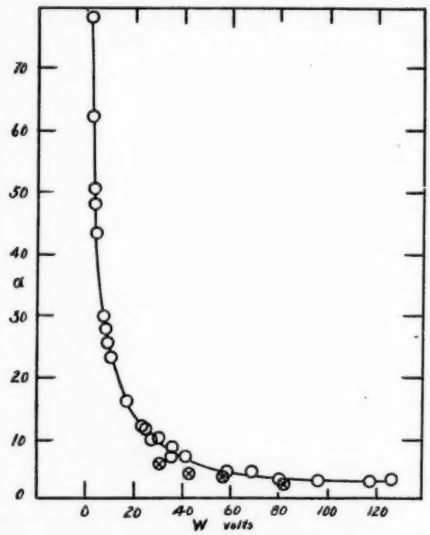

FIG. 1. The effective cross-sectional area of helium for scattering H^+. The points marked with crosses are values reported by Ramsauer and co-workers.

Each of these two species also contains just two electrons.

The helium hydride ion HeH^+ is known to be formed by the passage of electrons through mixtures of helium and hydrogen. Bainbridge[5] has used it in determining the mass of the deuteron. Beach,[6] Coulson and Duncanson,[7] and Tō[8] have made quantum mechanical studies of HeH^+. Coulson and Duncanson give an equilibrium internuclear distance of 0.764 or 0.848A, depending on their assumption as to the nature of the bond, and an interaction energy lying between 0.61 and 2.10 electron volts. Tō gives an interaction energy of 1.28 electron volts. Substitution of 0.8A in the above potential law gives 3.27 electron volts. High precision cannot be expected for this numerical result for two reasons. First, it is very sensitive to the assumed equilibrium distance; a distance of 1.1A, for example, gives 1.6 electron volts. Second, the classical potential law is assumed to hold down to the equilibrium distance; and even its experimental determination down to $r_a=0.8$A is not obtained with high precision. See Fig. 3.

For H_2^+ in He two potential laws are obtained. From 4 to 50 volts ($r_a=1.67$ to 0.87A) $\log Q=1.770$, $n=4$, and $K_e=1.47\times10^{-32}$.

$$V=-\frac{1.47\times10^{-32}}{r^4}. \tag{4}$$

From 50 to 120 volts ($r_a=0.87$ to 0.66A), $\log Q=1.735$ and $K_e=1.31\times10^{-32}$.

$$V=-\frac{1.31\times10^{-32}}{r^4}. \tag{5}$$

This is very nearly what would be expected on the basis of an interaction between a charge and a polarizable molecule. The polarizability α_P of helium[9] is 0.206×10^{-24}.

$$V_P=-\frac{\alpha_P Z^2e^2}{2r^4}=-\frac{1.483\times10^{-32}}{r^4}. \tag{6}$$

Above 50 volts ($r_a<0.87$A) the interaction is somewhat less, due perhaps to the appearance of repulsion. M'Ewen and Arnot[10] made a study of the formation of the helium hydride ion and found no evidence for the existence of HeH_2^+.

Three potential laws are found for the interaction of H_3^+ with He as seen in Fig. 3. From 1.5 to 14 volts ($r_a=2.22$ to 1.59A), $\log Q=1.790$, $n=6.68$, $K_a=6.17\times10^{-53}$, and $f=0.63$.

$$V=-\frac{3.9\times10^{-53}}{r^{6.68}}. \tag{7}$$

In evaluating K a long and questionable extrapo-

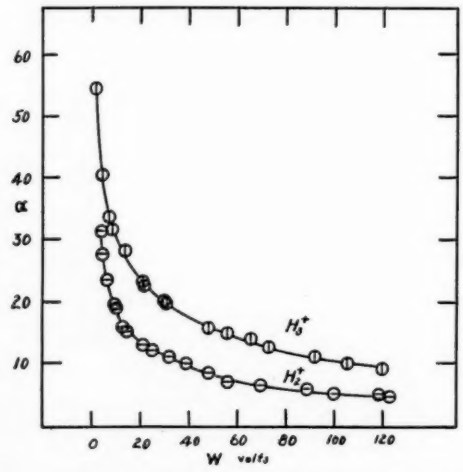

FIG. 2. The effective cross-sectional area of helium for scattering H_2^+ and H_3^+.

[5] K. T. Bainbridge, Phys. Rev. **44**, 57 (1933).
[6] J. Y. Beach, J. Chem. Phys. **4**, 353 (1936).
[7] C. A. Coulson and W. E. Duncanson, Proc. Roy. Soc. **A165**, 90 (1938).
[8] Sōroku Tō, Proc. Phys. Math. Soc. Japan **22**, 119 (1940).
[9] H. R. Hassé, Proc. Camb. Phil. Soc. **26**, 542 (1930).
[10] B. M'Ewen and F. L. Arnot, Proc. Roy. Soc. **A172**, 107 (1939).

lation is made of Fig. 5. From 14 to 65 volts ($r_a=1.59$ to 1.12A) $\log Q=1.960$, $n=4.46$, $K_a=1.50\times10^{-35}$, and $f=0.705$.

$$V=-\frac{1.06\times10^{-35}}{r^{4.46}}. \tag{8}$$

From 65 to 135 volts ($r_a=1.12$ to 0.89A), $\log Q=2.352$, $n=3.01$, $K_a=6.16\times10^{-24}$, and $f=0.783$.

$$V=-\frac{4.83\times10^{-24}}{r^{3.01}}. \tag{9}$$

ANALYTICAL TREATMENT OF THE SCATTERING PROBLEM AND EVALUATION OF f

The General Case

The method of evaluating K will follow the pattern of that used for the approximate treatment,[1] and the symbols used have the same definitions. First the beam intensity equation,

$$dI_T=INP\pi b^2dx \tag{10}$$

is integrated to give,

$$\ln\frac{1}{R}=Pl\alpha=NP\pi\int_0^l b^2dx, \tag{11}$$

since $\alpha=N\pi b^2$. The reason for the replacement of r_0 by b will be seen in Fig. 4 and the analysis below. Then, b^2 is expressed as a function of W, n, K, m_1, m_2, and the dimensions of the apparatus. The integration of $\int_0^l b^2dx$ combined with Eq. (11) will give the desired relationships.

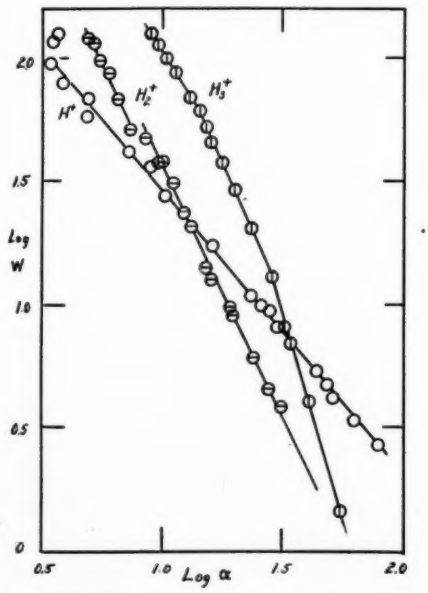

FIG. 3. H^+, H_2^+, and H_3^+ in helium.

We can consider a particle of mass, m_1, moving with an initial velocity v_0 past a molecule of mass, m_2, Fig. 4. The latter may be considered at rest if the reduced mass, $\mu=m_1m_2/(m_1+m_2)$, is used for m_1. The closest distance of approach, if there were no deflection, is b, and the perihelion distance is r_0. The angle of scattering relative to m_2 is θ.

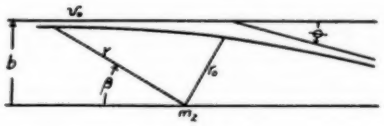

FIG. 4.

The laws of conservation of angular momentum and of energy for this system are $\mu r^2\dot\beta=\mu v_0b$ = constant and $E=\frac{1}{2}(\mu\dot r^2+r^2\dot\beta^2)-K/r^n=\frac{1}{2}\mu v_0^2$ = constant, for a potential law of the form of Eq. (1). Eliminating $\dot\beta$ from the above,

$$\dot r^2=\frac{E+(K/r^n)-(Eb^2/r^2)}{\frac{1}{2}\mu} \tag{12}$$

or

$$\frac{dr}{d\beta}=\frac{r^2}{b}\left(1+\frac{K}{Er^n}-\frac{b^2}{r^2}\right)^{\frac{1}{2}} \tag{13}$$

and as $\dot r=0$ when $r=r_0$ from (12)

$$b^2=r_0^2+\frac{K}{E}r_0^{2-n}. \tag{14}$$

The total increase in β during the entire collision will be $\pi+\theta$, hence

$$\pi+\theta=2\int_{r_0}^{\infty}\left(\frac{d\beta}{dr}\right)dr=2b\int_{r_0}^{\infty}\frac{dr}{r^2\left(1+\frac{K}{Er^n}-\frac{b^2}{r^2}\right)^{\frac{1}{2}}}. \tag{15}$$

If $y=r_0/r$, $dr/r=-dy/y$. Let $S_n=K/Er_0^n$. Using these relationships and the value of b from Eq. (14),

$$\theta=-\pi+2(1+S_n)^{\frac{1}{2}}\int_0^1[S_ny^n-(1+S_n)y^2+1]^{-\frac{1}{2}}dy. \tag{16}$$

Since $E=W(\mu/m_1)$, $S_n=(K/W)(m_1/\mu r_0^n)$. r_0 is, therefore, a function of W, K, θ, m_1, and m_2. As θ is a function of ϕ, the minimum angle of scattering relative to the apparatus, and the other parameters, and since $\tan\phi=a/(l-x)$, b^2

from Eq. (14) is now expressed as a function of x and the parameters. This enables the integral $\int_0^l b^2 dx$ to be expressed as a function of the desired quantities. Below, this is evaluated for certain cases.

The case $n=4$

Equation (16) for $n=4$ becomes,

$$\theta=-\pi+2(1+S_4)^{\frac{1}{2}}\int_0^1[(1-S_4y^2)(1-y^2)]^{-\frac{1}{2}}dy. \tag{17}$$

This integral is expanded in the following series by Jahnke and Emde.[11] S_4 must be less than 1.

$$\frac{\pi}{2}\left[1+2\frac{S_4}{8}+9\left(\frac{S_4}{8}\right)^2+50\left(\frac{S_4}{8}\right)^3+\frac{1225}{4}\left(\frac{S_4}{8}\right)^4+\cdots\right]$$

A relationship between θ and ϕ has been derived on the basis of the conservation laws and the assumption that the mass m_2 is initially at rest.[12]

$$\cot\phi=\cot\theta+\frac{m_1}{m_2}\csc\theta. \tag{18}$$

From Eq. (14)

$$\int_0^l b^2dx=\int_0^l r_0^2dx+\frac{K}{E}\int_0^l r_0^{-2}dx. \tag{19}$$

Since $\frac{dx}{a}=-d\cot\phi$ and $r_0^4=\frac{K}{W}\frac{m_1}{\mu}\frac{1}{S_4}$,

$$\int_0^l b^2dx=a\left(\frac{K}{W}\frac{m_1}{\mu}\right)^{\frac{1}{2}}\int_0^{l/a}S_4^{-\frac{1}{2}}d\cot\phi+a\left(\frac{K}{W}\frac{m_1}{\mu}\right)^{\frac{1}{2}}\int_0^{l/a}S_4^{\frac{1}{2}}d\cot\phi=a\left(\frac{K}{W}\frac{m_1}{\mu}\right)^{\frac{1}{2}}(A+B). \tag{20}$$

The integrals A and B can be evaluated graphically and separately for each value of the mass ratio, m_1/m_2, by substituting values for S_4 in the integrated form of Eq. (17). The values of θ thus obtained and Eq. (18) give values of $\cot\phi$ which may be plotted. From Eqs. (11) and (20)

$$\alpha W^{\frac{1}{2}}=\frac{a\pi N}{l}\left(\frac{m_1}{\mu}\right)^{\frac{1}{2}}K_e^{\frac{1}{2}}(A+B)=Q=\alpha W^{2/n}. \tag{21}$$

As

$$\alpha W^{2/n}=\pi^{\frac{1}{2}}N\left(\frac{l}{3a}\right)^{\frac{1}{2}}K_a^{\frac{1}{2}} \tag{22}$$

from the general approximate treatment[1]

$$\frac{K_e}{K_a}=\frac{\pi}{3}\left(\frac{l}{a}\right)^3\frac{\mu}{m_1}(A+B)^{-2}=f_e. \tag{23}$$

Values of f_e are shown in Table IV, and as points represented by crosses in Fig. 5. K_e and f_e refer to this exact treatment.

The case $n=4$ simplified

In the above, a plot must be drawn for every value of the mass ratio. If the assumption is made that the angle θ is small, only one plot will be needed and the different numerical values will be obtained from different limits set on this plot. If θ is small,

$$\cot\theta=\csc\theta, \quad \text{and} \quad \cot\phi=\frac{m_1}{\mu}\cot\theta=\frac{l-x}{a}. \tag{24}$$

Now

$$\int_0^l b^2dx=a\left(\frac{K}{W}\right)^{\frac{1}{2}}\left(\frac{m_1}{\mu}\right)^{\frac{1}{2}}\int_0^{\mu l/m_1a}S_4^{-\frac{1}{2}}d\cot\theta+a\left(\frac{K}{W}\right)^{\frac{1}{2}}\left(\frac{m_1}{\mu}\right)^{\frac{1}{2}}\int_0^{\mu l/m_1a}S_4^{\frac{1}{2}}d\cot\theta \tag{25}$$

$$=a\left(\frac{K}{W}\right)^{\frac{1}{2}}\left(\frac{m_1}{\mu}\right)^{\frac{1}{2}}(A_0+B_0). \tag{26}$$

$$\alpha W^{\frac{1}{2}}=N\pi\frac{a}{l}K^{\frac{1}{2}}\left(\frac{m_1}{\mu}\right)^{\frac{1}{2}}(A_0+B_0)=\alpha W^{2/n}. \tag{27}$$

$$f=\frac{K}{K_a}=\frac{\pi}{3}\left(\frac{l\mu}{am_1}\right)^3(A_0+B_0)^{-2}. \tag{28}$$

The values of f thus obtained are given in Table IV and plotted in Fig. 5. It is seen that the difference between f and f_e for the cases calculated is not significant in terms of the precision of the experiments. For values of n much greater than 4 and for values of m_1/m_2

[11] E. Jahnke and F. Emde, *Tables of Functions* (Steckert, New York, 1938).
[12] L. A. Pars, Phil. Mag. **33**, 96 (1942).

greater than $\frac{3}{2}$ the difference between these two quantities may become significant.

The case $n=2$

Equation (16) for $n=2$ becomes,

$$\theta=-\pi+2(1+S_2)^{\frac{1}{2}}\int_0^1(1-y^2)^{-\frac{1}{2}}dy. \quad (29)$$

When integrated,

$$\theta=-\pi+\pi(1+S_2)^{\frac{1}{2}}. \quad (30)$$

$$r_0^2=b^2-\frac{K}{W}\frac{m_1}{\mu}. \quad (31)$$

From Eq. (24)

$$dx=-a\frac{m_1}{\mu}d\cot\theta.$$

$$\int_0^l b^2dx=\int_0^{(l/a)(\mu/m_1)}ab^2\frac{m_1}{\mu}d\cot\theta=\frac{K}{W}\left(\frac{m_1}{\mu}\right)^2D, \quad (32)$$

where

$$D=\int_0^{(l/a)(\mu/m_1)}b^2\frac{W}{K}\frac{\mu}{m_1}d\theta. \quad (33)$$

In order to evaluate D, numerical values of $\cot\theta$ are found from values of θ obtained from the combination of Eqs. (30) and (31).

$$\theta=-\pi+\pi\left(1-\frac{m_1}{\mu}\frac{K}{W}\frac{1}{b^2}\right)^{-\frac{1}{2}}. \quad (34)$$

Values of $[(m_1/\mu)(K/W)(1/b^2)]$ are assumed for the calculations.

$$\alpha W=N\pi\frac{a}{l}K\left(\frac{m_1}{\mu}\right)^2D=\alpha W^{2/n}. \quad (35)$$

As

$$\alpha W^{2/n}=\frac{\pi^2Nl}{4a}K_a,$$

$$f=\frac{K}{K_a}=\frac{\pi}{4D}\left(\frac{\mu}{m_1}\frac{l}{a}\right)^2. \quad (36)$$

TABLE IV. The correction factor, f.

$\frac{m_1}{m_2}$	f $n=1$	f $n=2$	f $n=4$	f_c $n=4$
0	0.996	0.922	0.827	0.827
$\frac{1}{4}$	0.994	0.902	0.790	
$\frac{1}{2}$	0.992	0.882	0.756	0.760
$\frac{3}{4}$	0.989	0.862	0.725	0.731
1	0.985	0.843	0.696	
$\frac{3}{2}$	0.978	0.806	0.643	0.658

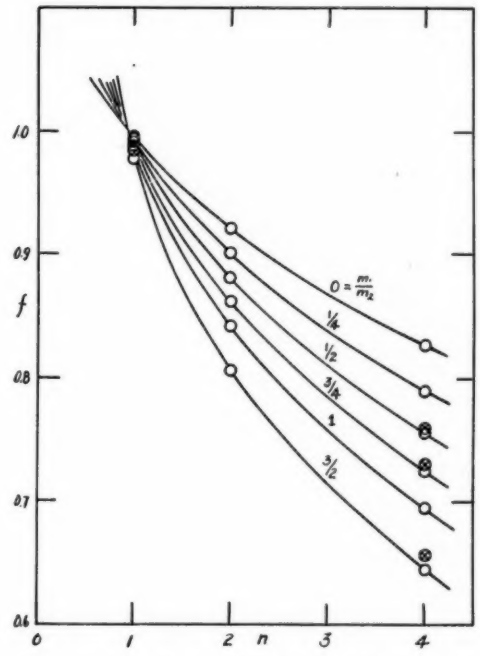

FIG. 5. The correction factor.

The values thus obtained for f are given in Table IV and plotted in Fig. 5.

The case $n=1$

Equation (16) for $n=1$ becomes

$$\theta=-\pi+2(1+S_1)^{\frac{1}{2}}\int_0^1[S_1y-(1+S_1)y^2+1]^{-\frac{1}{2}}dy. \quad (37)$$

Integrating and collecting terms give

$$\theta=-4\pi+2\sin^{-1}\left(\frac{S_1}{S_1+2}\right),$$

or

$$\sin\frac{\theta}{2}=\frac{S_1}{S_1+2} \quad (38)$$

for $n=1$,

$$S_1=\frac{m_1}{\mu}\frac{K}{Wr_0};\quad\text{and}\quad b^2=r_0^2+\frac{m_1K}{\mu W}r_0. \quad (39)$$

r_0 may now be eliminated from Eq. (38) and b^2 expressed in terms of θ, for

$$\sin\frac{\theta}{2}=\frac{1}{1+2/S_1}=\left[1+\left(2b\frac{\mu}{m_1}\frac{W}{K}\right)^2\right]^{-\frac{1}{2}}, \quad (40)$$

or

$$b^2=\left(\frac{m_1K}{2\mu W}\right)^2\frac{(1+\tan^2\theta)^{\frac{1}{2}}+1}{(1+\tan^2\theta)^{\frac{1}{2}}-1}. \quad (41)$$

Assuming θ is small,

$$\tan\theta=\frac{m_1}{\mu}\tan\phi=\frac{m_1 a}{\mu(l-x)}=v. \tag{42}$$

$$\int_0^l b^2dx=\left(\frac{m_1K}{2\mu W}\right)^2\frac{am_1}{\mu}\int_{m_1a/\mu l}^{\infty}\frac{(1+v^2)^{\frac{1}{2}}+1}{(1+v^2)^{\frac{1}{2}}-1}\frac{dv}{v^2} \tag{43}$$

$$=\left(\frac{m_1K}{2\mu W}\right)^2\frac{am_1}{\mu}\left[-\frac{2}{3}+\frac{2}{3}\left(\frac{l\mu}{am_1}\right)^3+\frac{l\mu}{am_1}+\frac{2}{3}\left(\frac{l\mu}{am_1}\right)^3\left(1+\frac{a^2m_1^2}{l^2\mu^2}\right)^{\frac{1}{2}}\right], \tag{44}$$

$$\alpha W^2=\alpha W^{2/n}=\frac{\pi N}{l}\left(\frac{m_1K}{2\mu}\right)^2\frac{am_1}{\mu}\left[\begin{matrix}\text{same}\\ \text{as in}\\ (44)\end{matrix}\right]. \tag{45}$$

As

$$\alpha W^{2/n}=\frac{\pi N}{3}\left(\frac{l}{a}\right)^2K_a, \tag{46}$$

$$f=2\left[-2\left(\frac{am_1}{l\mu}\right)^3+2+3\left(\frac{am_1}{l\mu}\right)^2+2\left\{1+\left(\frac{am_1}{l\mu}\right)^2\right\}^{\frac{3}{2}}\right]^{-\frac{1}{3}}. \tag{47}$$

Values of f are found in Table IV and are plotted in Fig. 5.

The case $n=0$

Equation (16) becomes

$$\theta=-\pi+2(1+S_0)^{\frac{1}{2}}\int_0^1[S_0-(1+S_0)y^2+1]^{-\frac{1}{2}}dy, \tag{48}$$

where $S_0=m_1K/\mu W$.

$$\theta=-\pi+2\int_0^1(1-y^2)^{-\frac{1}{2}}dy$$

$$=-\pi+2\left(\frac{\pi}{2}-0\right)=0. \tag{49}$$

This would be expected as V is independent of r.

If $\theta=0$, $\phi=0$. The approximate treatment gives $\tan\phi=KC/Wr_0^n$; and for $n=0$, $\tan\phi=0$ and $\phi=0$. Thus for $n=0$ the exact and approximate treatment gives the same result.

The value of n

It is seen that in each case the value of n obtained by the approximate method is exactly equal to that arrived at with more exact analyses. This is very satisfactory as the value of n is more significant than the value of K and it is obtained correctly directly from a logarithmic plot of the experimental data.

THE JOURNAL OF CHEMICAL PHYSICS VOLUME 11, NUMBER 7 JULY, 1943

Infra-Red Absorption of Pyridine Vapor

JOHN TURKEVICH AND PETER COOPER STEVENSON
Frick Chemical Laboratory, Princeton University, Princeton, New Jersey

(Received May 14, 1943)

The determination of the infra-red spectrum of pyridine vapor was of interest in this laboratory since its knowledge was necessary for the calculation of thermodynamic functions for possible pyridine syntheses. The spectrum for the liquid was measured by Coblentz and by LeCompte. These measurements, however, were carried on samples of unknown purity and the use of the results for frequency assignment is vitiated by the fact that selection rules which discriminate between various types of molecular vibrations, do not hold rigorously for molecules in the liquid state. The determination of the infra-red absorption spectrum was, therefore, carried out on a carefully purified sample of pyridine in the vapor state.

EXPERIMENTAL

THE infra-red spectrometer was a rocksalt prism instrument of the Wadsworth type described by Barnes.[1] The pyridine samples were transferred in a vacuum system at known pressures into a cylindrical Pyrex absorption cell fitted with rocksalt windows. The optical length of the cell was 224 mm. The absorption cell was raised and lowered, in and out of the light beam, readings being taken at each wave-length.

The pyridine was purified according to the procedure of Heap, Jones, and Speakman.[2] The

[1] Barnes, Brattain, and Seitz, Phys. Rev. **48**, 582 (1935).

[2] Heap, Jones, and Speakman, J. Am. Chem. Soc. **43**, 1936 (1921).

TABLE I. Absorption maxima in cm^{-1}.

Pyridine			Benzene			
Vapor	Liquid		Vapor	Vapor	Liquid	Slit width used
T S	C	L	T S	BHIT	BHIT	T S
3070s	3077s		3060s	3098s	3070s	47
				3061s		
				2857w		
			2665m		2629m	32
				2288w	2290s	
1991m			1975s	1965s	1963s	
	1923m			1906vw		13
1830s			1812s	1808s	1810s	
	1723m					
					1669s	
1605s	1600s			1617w	1604s	13
					1584s	
1510s			1500s	1497s		
1481s	1481s			1485s	1480s	
				1474s		
1445s	1439s					7
	1369m		1394s	1377w	1381m	
			1285m		1298w	
	1211s		1248w	1240vw		7
		1190w			1170s	
	1138s	1125w	1135m	1143w		
	1069s	1052w		1048s		
1037s	1028s	1020s	1037s	1037s	1033s	5
				1026s		
	992s	984s				
	886m	890m				
					849s	
	806m	811m				
			783m		773s	
	751s	746s				
690s	709s	708s	690s	684s	685s	
669i			671s	671s		5
662s		601s	660s	658s	658s	

TS = our measurements.
C = measurements of Coblentz.
L = measurements of LeCompte.
BHIT = measurements of Bailey, Hale, Ingold, and Thompson, J. Chem. Soc. **1936**, 931 (1936).
s = strong, m = medium, w = weak absorption, and i = inflection.

purification involved careful distillation, triple crystallization of the zinc chloride salt from absolute alcohol, decomposition of the salt with sodium hydroxide and a final rectification. All precautions were taken to eliminate the absorption of atmospheric moisture by the sample. The benzene used was dried, thiophene free, reagent grade benzene.

RESULTS

Figure 1 presents the infra-red spectrum of pyridine vapor and that of benzene vapor. The latter was taken for comparison and as an additional check on the calibration of the spectrometer. Table I presents measurements of the absorption bands for the pyridine and benzene vapors and the measurements of other workers on pyridine and benzene.

The agreement of the benzene data with that

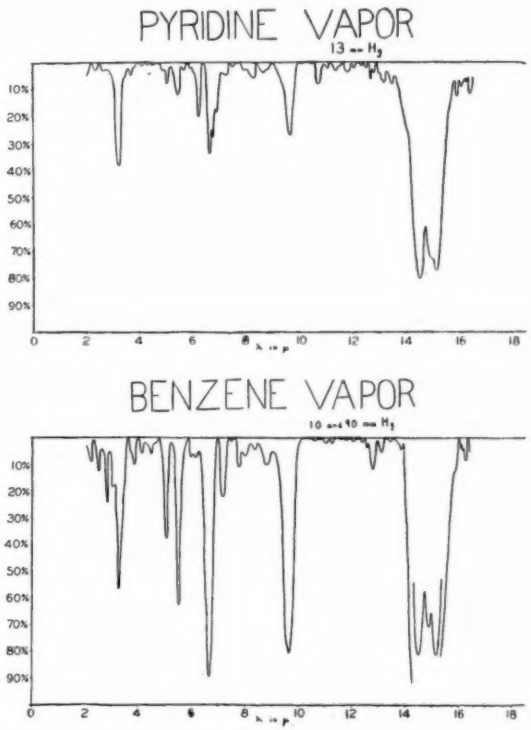

FIG. 1.

reported by Bailey, Hale, Ingold, and Thompson is satisfactory in view of the superior spectrometer available to the British investigators. The data on the pyridine vapor differs in many respects from that reported for the liquid by Coblentz[3] and LeCompte.[4] Neither of these workers reported the strong bands at 1830 and 1510 cm^{-1}, nor do the following bands, which they reported for the liquid, exist in the vapor: 1923, 1723, 1369, 1211, 1138, 1069, 992, 886, 806, and 751 cm^{-1}. This serves as an illustration of the fact that strong bands in the liquid do not necessarily occur in the vapor. A similar phenomenon has been noted by Bailey, Hale, Ingold, and Thompson for benzene.

The frequency assignment on the basis of this, the Raman and the fluorescence data, and the use of such an assignment for thermodynamic calculations are subjects of a subsequent communication from this laboratory.

We wish to thank Professors H. D. Smyth and L. G. Smith for extending to us the facilities of the Palmer Physics Laboratory.

[3] Coblentz, *Investigations of Infra-Red Spectra, Part I* (Carnegie Institute of Washington Publications, 1905).
[4] LeCompte, Comptes rendus **207**, 395 (1938).

The Structure of Liquid Mercury

J. A. CAMPBELL AND J. H. HILDEBRAND
Department of Chemistry, University of California, Berkeley, California

(Received April 26, 1943)

The structure of liquid mercury has been determined by means of the diffraction of monochromatic molybdenum $K\alpha$ x-radiation at $-38°$, 0°, 50°, 100°, 150°, and 200° C. The position of the first peak remains quite constant at 3.00A but the number of atoms in this first coordination layer varies between 6.0 and 5.3, giving the lowest coordination number yet found for any monatomic element in its normal liquid range.

MERCURY was one of the first liquids to be studied by means of x-ray diffraction methods and has been frequently investigated since the first attempt was made by Wyckoff [1] in 1923. Although at least nine independent investigations[1–9] have been made of the x-ray diffraction patterns of the liquid none of the previous researches has been sufficiently complete either from an experimental or analytical standpoint to give an unambiguous picture of the arrangement of the atoms in the liquid. Only Gingrich and Gamertsfelder used strictly monochromatic radiation and hence all the patterns save theirs are subject to serious doubt as has been pointed out by Gregg and Gingrich.[10] However, Gingrich and Gamertsfelder worked only at room temperature and have not analyzed their intensity curves to obtain the more interesting distribution curves of the atoms in the liquid.

EXPERIMENTAL

The x-rays were generated in a commercial model General Electric tube with a molybdenum target run at 30 kvp and 20 ma. The radiation from the tube was collimated by passage through a slit block 5 cm long with slit dimensions 1.20 $\times$0.02 cm. The collimated beam was incident on a rocksalt crystal set for reflection of the Mo $K\alpha$ line. This monochromatic beam impinged on the surface of the sample and was diffracted by it. The angle of incidence of the x-ray beam to the horizontal surface of the sample was 4° 45′.

The mercury was held in a shallow iron tray mounted on a copper block. The copper block could be cooled or heated and the temperature of the mercury was determined by means of a copper-constantan thermocouple placed about 2 mm below the irradiated mercury surface. Temperature control was maintained within $\pm$1°C at all temperatures.

At the higher temperatures a thin layer of oxide formed on the mercury surface. This prevented evaporation of the sample and was allowed to remain. The x-ray diffraction lines from this layer were easily subtracted from the total diffraction pattern. Frost formation at the lower temperatures and entry of mercury vapor into the camera at the higher temperatures were prevented by blowing a stream of dry air through the camera and over the sample.

The camera was the one used by Boyd and Wakeham[8] with minor changes in the amount of shielding to prevent secondary radiation striking the film. A nickel filter 0.033 mm thick was interposed halfway between the sample and the film. The effective radius of curvature of the camera was 7.00 cm.

Agfa Non-Screen X-ray Safety Film[11] was used throughout and was developed for five minutes in Eastman X-ray Developer D-19. The films were hardened in an acid hardener bath, dried

[1] R. W. G. Wyckoff, Am. J. Sci. **5**, 455 (1923).
[2] C. V. Raman and C. M. Sogani, Nature **120**, 514 (1927); Ind. J. Physics **2**, 97 (1927–28).
[3] J. A. Prins, Physica **6**, 315 (1926).
[4] M. Wolf, Nature **122**, 314 (1928); Zeits. f. Physik **53**, 72 (1929).
[5] P. Debye and H. Menke, Physik. Zeits. **31**, 348 (1930).
[6] F. Sauerwald and W. Teske, Zeits. f. anorg. allgem. Chemie **210**, 247 (1933).
[7] V. I. Danilow and V. E. Neimark, J. Expt. and Theoretical Physics, U. S. S. R. **5**, 724 (1935).
[8] R. N. Boyd and H. R. R. Wakeham, J. Chem. Phys. **7**, 958 (1939).
[9] N. S. Gingrich and C. Gamertsfelder, private communication.
[10] R. Q. Gregg and N. S. Gingrich, Rev. Sci. Inst. **11**, 305 (1940).
[11] C. Gamertsfelder and N. S. Gingrich, Rev. Sci. Inst. **9**, 154 (1938).

and microphotometered. Density was converted into intensity in the usual manner.

CALCULATIONS

The method of analysis and the mathematical theory upon which it is based have been discussed by Warren and Gingrich.[12] The fundamental equation is

$$4\pi r^2\rho(r)=4\pi r^2\rho_0+2r/\pi\int_0^\infty si(s)\sin rs\,ds \quad (1)$$

where $4\pi r^2\rho(r)dr$ is the actual number of atomic centers in a spherical shell of radii r and $r+dr$ measured from an atom at the center of the sphere, $4\pi r^2\rho_0 dr$ is the number of atomic centers in a similar shell assuming the liquid to be a continuum of atomic density ρ_0. $s=4\pi(\sin\theta)/\lambda$, and $i(s)=(I/N-F^2)/F^2$. Here F is the atomic structure factor, and I/N is the coherent scattering per atom in the liquid. I/N was obtained from the experimental intensity curve by correcting the experimental intensities for absorption, polarization and incoherent scattering of x-rays by the sample and setting the experimental intensity equal to the calculated coherent intensity at some large value of s through multiplying the experimental intensity at that point by a suitable factor, q. Each value of the experimental curve was then multiplied by q to give a curve of I/N as a function of s. The terms necessary for the calculation of the coherent and incoherent scattering curves are available in tabular form.[13]

The integral in Eq. (1) was evaluated using the method of trigonometric interpolation devised by Lanczos and Danielson[14] to yield the radial distribution curve of the liquid.

RESULTS

Runs were made at −38°, 0°, 50°, 100°, 150°, and 200° C. The intensity curves obtained are shown in Fig. 1. The experimental curves have been corrected for absorption, polarization and incoherent scattering of x-rays by the sample and have been converted into electron units by matching with the F^2 curve at $s=9.00$. Table I gives a comparison of the results of this research with those of previous workers insofar as is possible through a mere listing of peak positions. That such a comparison is not sufficient is well illustrated by the work on argon in which the peak positions in the intensity curves agree well but the distribution curves are different.[15–17]

The distribution curves are given in Fig. 2 and a summary of the data obtainable from them in Table II. There are two general methods for determining the number of atoms in a given coordination layer. In one the area to be integrated is bounded by perpendiculars drawn to the r axis from the minima in the experimental radial distribution curve. This method cuts off each coordination layer at a sharp value of r. The other method bounds the area by symmetrical peaks obtained from the distribution

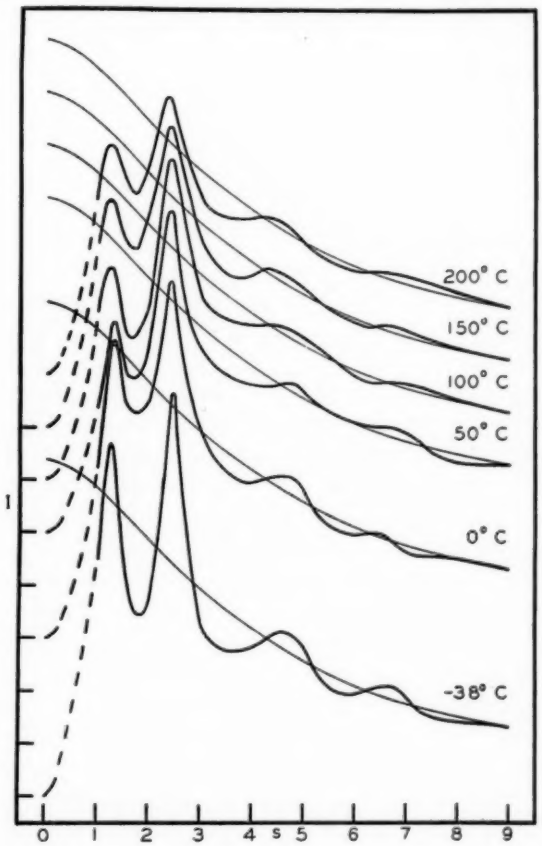

FIG. 1.

[12] B. E. Warren and N. S. Gingrich, Phys. Rev. **46**, 368 (1934).

[13] A. H. Compton and S. K. Allison, *X-Rays in Theory and Experiment* (D. van Nostrand and Company, Inc., 1935), p. 780–782.

[14] C. Lanczos and G. C. Danielson, Phys. Rev. **55**, 242 (1939).

[15] K. Lark-Horovitz and E. P. Miller, Nature **146**, 459 (1940).

[16] A. Eisenstein and N. S. Gingrich, Phys. Rev. **58**, 307 (1940).

[17] A. Eisenstein and N. S. Gingrich, Phys. Rev. **62**, 261 (1942).

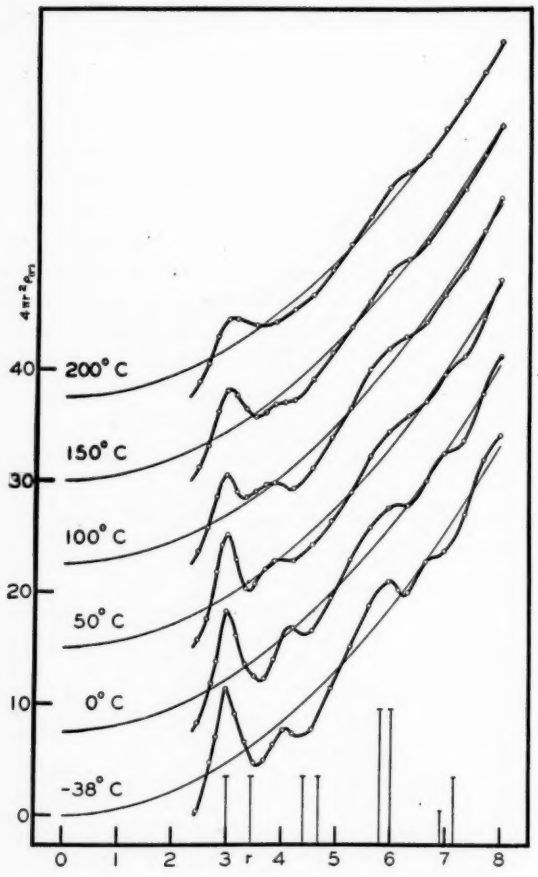

FIG. 2.

curve and thus allows various degrees of overlapping of the several coordination layers. The first peak is made symmetrical about the first maximum and the initial rise in the distribution curve and the rest of the peaks are determined by subtracting this peak from the remainder of the distribution curve, etc. The first method allows the calculations to be made much more readily as each is fairly independent of the others, while any error made in determining the number of neighbors in the first coordination shell by the second method is multiplied in the succeeding calculations. The results of both methods are listed in Table II for the first coordination layer but the other peaks are evaluated by dropping perpendiculars from the corresponding minima. It will be noted that the trends are similar in the two evaluations though the values obtained are different. The numbers and positions of the atoms in the solid are given by the perpendicular lines along the r axis in Fig. 2.

TABLE I.

Experimenter	Peak position: (sin θ/λ) I	II	III	IV	Temp. (°C)	Ref.
Raman and Sogani		0.165				2
Prins		0.180	0.354	0.495		3
		0.176	0.344	0.460		
		0.171	0.358			
Debye and Menke		0.163	0.358	0.520		5
Sauerwald and Teske		0.152	0.346	0.438		6
Danilow and Neimark		0.195	0.344	0.485	−31°	7
		0.189	0.353	0.538	room	
		0.195	0.349	0.531	30°	
Boyd and Wakeham	0.136	0.220	0.37		−36°	8
	0.142	0.220	0.37	0.55	−34°	
	0.165	0.206	0.35		0°	
	0.115	0.195	0.335	0.535	30°	
	0.120	0.207	0.340		75°	
	0.115	0.210	0.405	0.56	125°	
	0.117	0.208	0.335		175°	
Gingrich and Gamertsfelder	0.118	0.184	0.37	0.52	room	9
This Research	0.099	0.195	0.364	0.53	−38°	
	0.103	0.191	0.366	0.51	0°	
	0.103	0.191	0.374	0.52	50°	
	0.099	0.191	0.354	0.53	100°	
	0.098	0.190	0.341	0.52	150°	
	0.099	0.187	0.334	0.51	200°	

TABLE II.

Temp.	r_{min}	Peak I* Pos.	Area I	Area II	Peak II Pos.	Area	Peak III Pos.	Peak IV Pos.
−38°	2.40	3.00	6.7	6.0	4.08	5.0	6.0	6.7
0°	2.36	3.00	6.7	5.8	4.17	6.0	6.1	6.9
50°	2.34	3.00	5.7	5.8	3.95	4.7	6.0	7.0
100°	2.32	3.00	4.4	5.5	3.85	5.8	6.0	—
150°	2.29	3.00	6.1	5.3	3.95	3.8	6.0	—
200°	2.24	3.05	7.0	5.9	—	—	6.2	—

* Column I under area of Peak I gives No. of neighbors obtained by dropping perpendiculars, and column II gives No. obtained by method of symmetrical peaks.

In Fig. 3 we present the W function of Menke which shows the probability of finding an atomic center in the interval r to $r+dr$ from the central atom, based on an average probability of one if the liquid were a continuum.

DISCUSSION

While a good many experimenters, Table I, have obtained diffraction curves from liquid mercury, only two previous attempts have been made to analyze these patterns into a structural representation. Debye and Menke give a plot of their W function *vs.* r, while Boyd and Wakeham

give both the plots of the W function and the radial distribution curves. Debye and Menke did not observe the first maximum in the intensity curve at $s=1.30$ and hence obtain a W curve considerably different from those of this research. Boyd and Wakeham found intensity curves similar to those of this research but with the peaks shifted to higher values of s. This was presumably due to their use of filtered rather than reflected radiation. Thus their radial distribution curves do not agree with those of this work though having certain characteristics in common.

The first and second main peaks, at 3.0A and 5.7A, as might be expected, do not change positions appreciably as temperature is increased but become lower and broader. The small peak in the neighborhood of 4A, however, not only broadens but also shifts rapidly and finally disappears. This is the second case where the behavior of such a subsidiary peak has been accurately studied through a considerable range of temperature, the other being argon.[17] They have been observed in several other liquids, however.[18]

One might be tempted to regard these subsidiary peaks as illusory, since they are so small as to suggest experimental error and they do not correspond to any expected geometrical structure. However, their occurrence again and again with different liquids and independent investigators make them appear real. The physical magnitude of these peaks is such that it would disappear on movement of one atom. The only explanation we have to offer is that during an exchange of position of a pair between the first and second coordination shells the rapidity of the interchange would be least at the halfway point, since the potential between the two cages would here go through a maximum.

The behavior of the small peak in the neighborhood of 7A is analogous to that of the one at 4A save that the 7A one shifts to larger values of r with increase in temperature. Again, less than one atom is involved in the migration.

From a study of these curves it is possible to follow three definite trends in the structures of liquid mercury with temperature, all of them compatible with the usual conceptions of liquids. (1) The "toe" of the curve, r_{min}, in the neighborhood of 2.4A moves to slightly smaller distances as the temperature rises due to greater interpenetration of the electron shells of the atoms. (2) The structure of the liquid tends to smear out and approach a continuum as a limit with increasing temperature. The first peak remains, however, and becomes lower and broader in such a manner that approximately the same number of atoms remain in the first coordination layer. (3) The position of the "main" peaks does not shift greatly with temperature since it varies mainly with the cube root of the density while the "subsidiary" peaks tend to disappear completely with rising temperature, moving their peak position in the liquid an appreciable amount in so doing.

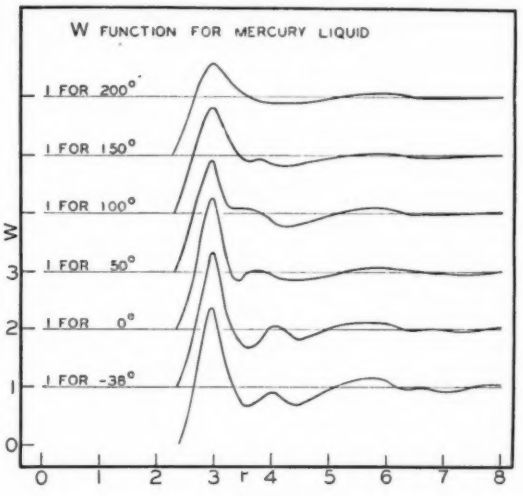

FIG. 3.

We had expected to publish a recalculation of the potential curve of mercury from these data, using the method of Hildebrand and Wood[19] as outlined by Hildebrand, Wakeham and Boyd[20] but have decided to postpone this till the end of the war.

ACKNOWLEDGMENT

The junior author wishes to express his thanks to the E. I. du Pont de Nemours Company, and to the Great Western Dow Chemical Company, for fellowships which allowed him to devote his time to this research.

[18] C. Gamertsfelder, J. Chem. Phys. **9**, 450 (1941).

[19] J. H. Hildebrand and S. E. Wood, J. Chem. Phys. **1**, 817 (1932).

[20] J. H. Hildebrand, H. R. R. Wakeham, and R. N. Boyd, J. Chem. Phys. **7**, 1094 (1939).

The Structure of Liquid Xenon

J. A. CAMPBELL AND J. H. HILDEBRAND
Department of Chemistry, University of California, Berkeley, California

(Received April 26, 1943)

The structure of liquid xenon has been investigated by means of the diffraction of monochromatic silver $K\alpha$ x-radiation. Patterns were obtained under three sets of conditions: (1) Temperature $-110°C$, pressure 1 atmos., specific volume 0.324 cc/g; (2) temperature $-90°C$, pressure 2.5 atmos., specific volume 0.339 cc/g; (3) temperature $-90°C$, pressure 130 atmos., specific volume 0.324 cc/g. The number of nearest neighbors varies from 9 to 10 and their distance from the central atom from 4.43A to 4.50A. It is found that, in liquid xenon, the structure is determined mainly by the specific volume, with the temperature giving a lesser effect.

THIS investigation of the x-ray scattering pattern of liquid xenon was undertaken in order to study the effect of variations in temperature and volume upon the structure of a monatomic, non-metallic liquid where, for the purpose of theoretical treatment, spherical symmetry and additive interatomic forces can be assumed. It was of particular interest to learn whether the structure could be treated, at least approximately, as a volume function. Although the structures of a number of metallic liquids have been reported, the only liquid thus far examined which satisfies the above criteria is argon. In this case we have the excellent data by Lark-Horovitz and Miller,[1] and by Eisenstein and Gingrich.[2,3] A theoretical treatment of the structure of such liquids has recently been published by Kirkwood and Boggs.[4]

EXPERIMENTAL

The x-rays were generated in a Purdue type x-ray tube[5] run at 33 kvp and 20 ma with a silver target. The radiation was collimated (see Fig. 1) by passing through a series of lead slits (8, 10, 11) to give a beam just sufficiently broad to completely bathe the cylindrical sample of xenon. A rocksalt crystal (9) was used to insure radiation of the sample by only the Ag $K\alpha$ line.

Figure 1 shows the general experimental arrangement of the camera and sample. The xenon was frozen into the thin-walled glass capillary (6) by filling the Dewar vessel (1) with liquid air, pumping a vacuum in the camera, and allowing the cold vapors from the boiling liquid air to leak down past the capillary. This gas leak was adjusted by placing glass rods of various fits in the glass tube (3) above the capillary. In this way it was possible to maintain a vacuum of a centimeter or less in the camera and still get efficient cooling of the sample. A thin cylinder of Cellophane (4) was cemented to the lower end of the tube delivering the cold gas to the camera and extended down past the thermocouple junction point (7) on the capillary. This prevented convection currents warming up the sample and forced all the cold gas entering the camera to pass by the capillary and thermocouple.

The thermocouple was connected through a potentiometer to a galvanometer from whose mirror light was reflected onto two photo-cells, equally when the temperature was at the desired value. If the temperature rose above this value one of the photo-cells received more illumination and opened a compressed air jet connected to a fifty-liter Dewar containing the supply of liquid air. When sufficient liquid air had been blown from the reservoir into the glass Dewar atop the camera so that the temperature returned to the desired value the galvanometer swung back and illuminated the second photo-cell, turning off the compressed air and opening a venting valve which immediately stopped the flow of liquid air into the small Dewar. This device was able to keep the temperature constant throughout the range of $-190°C$ to $-10°C$ within $\pm 1°C$.

[1] K. Lark-Horovitz and E. P. Miller, Nature **146**, 459 (1940).
[2] A. Eisenstein and N. S. Gingrich, Phys. Rev. **58**, 307 (1940).
[3] A. Eisenstein and N. S. Gingrich, Phys. Rev. **62**, 261 (1942).
[4] J. G. Kirkwood and E. M. Boggs, J. Chem. Phys. **10**, 394 (1942).
[5] K. Lark-Horovitz and E. P. Miller, Rev. Sci. Inst. **4**, 379 (1933).

For the high pressure runs the steel needle valve (12) was closed and the mercury (from 13) rapidly run up into the capillary until the desired pressure was reached. Pressure was obtained from a cylinder of compressed nitrogen and was transmitted to the xenon through the mercury. The runs at 1 atmos. and at 130 atmos. were designed to give the same specific volume for the liquid xenon. In going from -110°C to -90°C the density and, hence, specific volume of the liquid xenon changes 4.3 percent. The liquid filled about four centimeters of the capillary so that the expansion linearly was 0.17 cm. After applying the high pressure the liquid xenon had returned to its shorter length within ± 0.02 cm as measured with a cathetometer. Therefore, the two determinations were at very nearly the same specific volume, though it can not be stated definitely that the actual pressure in the capillary was 130 atmos.

A cylindrical camera of 5.73 cm radius was used with a 0.002-inch Al window for entry of the x-rays, and a back window of 0.033-inch Ni (5) to minimize the amount of xenon characteristic radiation striking the photographic film.

New type Agfa Non-Screen X-ray Film was used exclusively.

CALCULATION

The theory and application of the analysis of the diffraction patterns has been given by Warren and Gingrich.[6] The fundamental equation is:

$$4\pi r^2\rho(r) = 4\pi r^2\rho_0 + 2r/\pi \int_0^\infty si(s) \sin rs\, ds. \quad (1)$$

$4\pi r^2\rho(r)dr$ is the actual number of atomic centers to be found on the average in the interval r to $r+dr$; $4\pi r^2\rho_0 dr$ is the number that would be found in the interval if the liquid had no structure; $s = 4\pi \sin\theta/\lambda$; and $i(s) = [(I_m - I_i)/I_e] - 1$. Here I_m is the experimental intensity corrected for absorption and polarization of the radiation by the sample and converted into electron units per atom, I_i is the incoherent scattering per atom, and I_e is the coherent scattering per atom. The values necessary for the calculation of I_i and I_e have been collected in tabular form.[7] The correction for absorption was applied as outlined by Blake[8] for a cylindrical sample and found to be quite small.

The evaluation of the integral in Eq. (1) was carried out by means of the method of trigonometric interpolation devised by Lanczos and Danielson.[9]

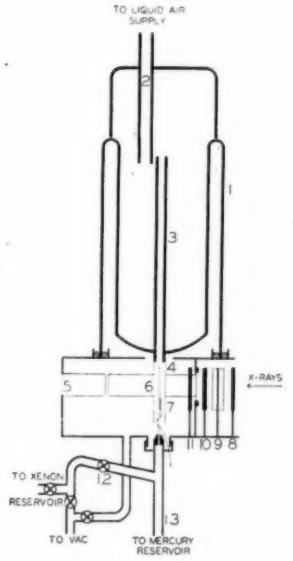

FIG. 1.

RESULTS

Runs were made under three sets of conditions: (1) at a temperature of -110°C and a pressure of 1 atmos., sp. vol. 0.324 cc/g, (2) at a temperature of -90°C and a pressure of 2.5 atmos., sp. vol. 0.339 cc/g and, (3) at a temperature of -90°C and a pressure of about 130 atmos., sp. vol. 0.324 cc/g. The intensity curves obtained are shown in Fig. 2. These intensities have been corrected for absorption and polarization and have been converted into electron units. The positions of the maxima in the intensity curves are listed in Table I. The radial distribution curves derived from these diffraction patterns are given in Fig. 3, while the number of neighbors and their average distance from the central atom are listed in Table II.

Two methods are in use for determining the number of atoms in any coordination layer as mentioned by us in our discussion of the structure

[6] B. E. Warren and N. S. Gingrich, Phys. Rev. **46**, 368 (1934).

[7] Compton and Allison, *X-Rays in Theory and Experiment* (D. van Nostrand and Company, Inc., 1935), p. 780–782.

[8] F. C. Blake, Rev. Mod. Phys. **5**, 169 (1933).

[9] C. Lanczos and G. C. Danielson, Phys. Rev. **55**, 242 (1939).

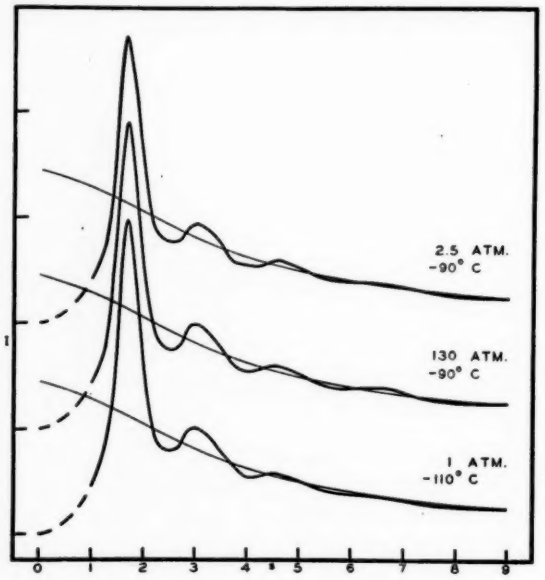

FIG. 2.

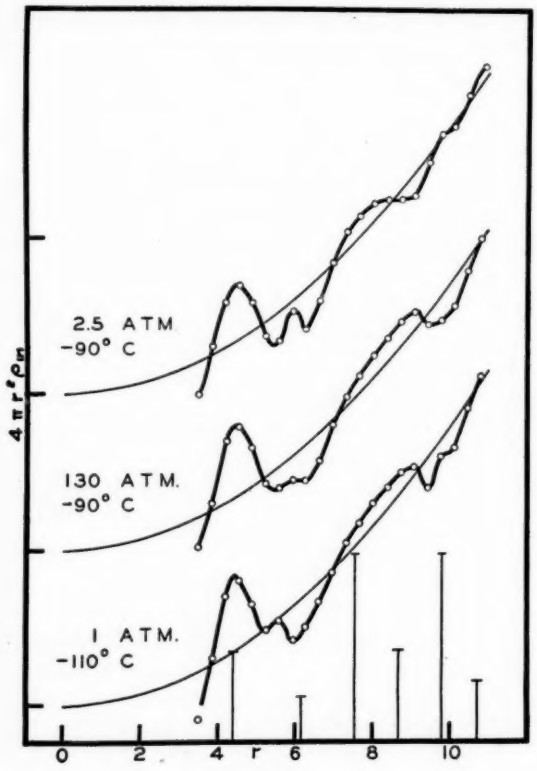

FIG. 3.

of mercury.[10] In one method the area to be integrated under the radial distribution curve is bounded by perpendiculars dropped from the minima in the distribution curve to the r axis. In the second method the areas are determined under symmetrical peaks. The results for both methods of calculating the number of atoms in the first coordination layer of the xenon are tabulated in Table II, but for the more distant neighbors the evaluation was made by method one. It is apparent that the trends in the two sets of evaluations are parallel though the figures are different. The numbers and positions of the various coordination neighbors in the solid are given in Fig. 3 by the lines perpendicular to the r axis.

Figure 4 presents the results in the form of Debye's W curve, which gives ρ_r/ρ_0 of Eq. (1) as a function of r. These show, in other words, the relative deviation of the actual liquids from a continuum. The W curve for the run at −90°C and 130 atmos. is superimposed on each curve for comparison.

DISCUSSION

From a comparison of the W curves for the three runs it is clear that the specific volume of the liquid xenon determines the shape and positions of the "main" peaks in the probability curve, while the effect of temperature is evident mainly in the subsidiary peaks. Thus at approximately equal specific volumes the peaks at 4.4A and 8A

TABLE I.

Temp.	Press.	Sp. Vol.	Peak I	Peak II	Peak III	Peak IV
−110	1	0.324	1.68(.134)	3.00(.239)	4.5(.36)	6.5(.52)
− 90	130	0.324	1.67(.133)	3.00(.239)	4.5(.36)	6.5(.52)
− 90	2.5	0.339	1.66(.132)	3.00(.239)	4.6(.37)	6.4(.51)

Temperature is in centigrade degrees, pressure in atmospheres, specific volume in cc/g. Position is given in terms of s (first figure) and $\sin\theta/\lambda$ (in parenthesis).

[10] J. A. Campbell and J. H. Hildebrand, J. Chem. Phys. **11**, 330 (1943).

TABLE II.

Temp.	Press.	r_{min}	Peak I Pos.	Peak I Area I	Peak I Area II	Peak II Pos.	Peak II Area	Peak III Pos.	Peak III Area	Peak IV Pos.	Peak IV Area
−110	1	3.60	4.43	9.4	8.5	5.55	3.5	9.1	38	9.9	—
− 90	130	3.45	4.47	10.1	9.0	5.95	3.4	9.1	38	—	—
− 90	2.5	3.50	4.50	9.0	8.3	5.95	3.6	8.0	28	9.8	—

Temperature is in centigrade degrees; pressure in atmospheres; r_{min} in A (gives distance of closest approach of atoms); position is in angstroms from central atom; and area in number of atoms in given coordination layer. For area determination under Peak I the figures in column I were obtained by dropping a perpendicular from the first minimum and those in column II by drawing a symmetrical peak.

are very nearly the same in the two curves, while the same two peaks at the larger specific volume have changed appreciably.

In raising the temperature from −110°C to −90°C the subsidiary peak at 5.5A moves out to 5.9A and separates from the main peak. If the specific volume is then reduced by increasing the pressure while keeping the temperature constant this small peak almost completely disappears but the small residue remains at the position which it held at the higher specific volume at that temperature.

The number of atoms in the first coordination layer varies but slightly with temperature but increases appreciably upon application of a large external pressure. This increase occurs at the expense of the layers farther out than 6A rather than at the expense of the small concentration around 5.5A. This increase is what would be expected if the atoms are forced farther apart (4.47A *vs.* 4.43A) at a given specific volume due to different degrees of thermal agitation while at the same time being forced to a higher average density by the larger pressure. This will account for no more than half the effect by itself, however.

It should be noted that the changes in structure with temperature are not nearly as pronounced with xenon as with argon even if reduced temperatures are used as a comparison, though a region of great similarity is passed through by each. (Reduced values are obtained by dividing the experimental values by the corresponding critical constant.) As a means of comparison of the two liquids we have plotted in Fig. 5 the W function for (1) xenon at 1 atmos. and −110°C, and (2) argon[3] at 1.8 atmos. and −181.3°C

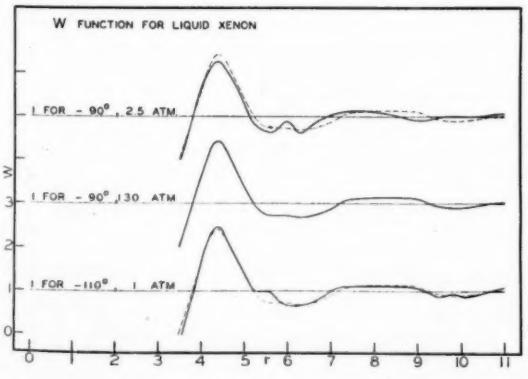

FIG. 4.

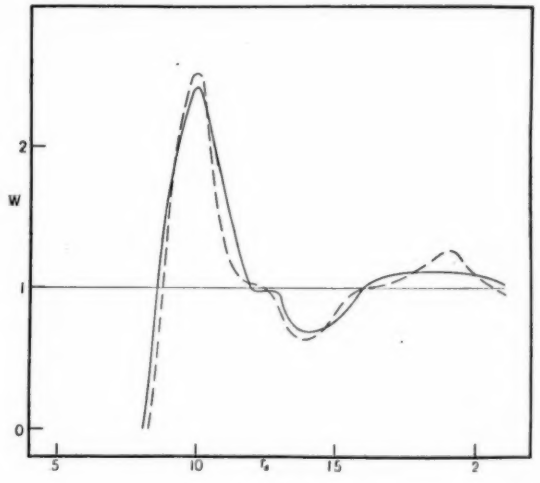

FIG. 5.

against a distance function r_d. Here r_d is defined as r/r_{max}, r_{max} being the value of r at which W is greatest for the liquid in question. For xenon the reduced volume is 0.375 and the reduced temperature 0.564 and for argon the reduced volume is 0.384 and the reduced temperature 0.604. These two curves were chosen to give a close fit but it is interesting that such a similarity exists. The fact that the reduced values must be greater in the case of argon may be attributed to the lower kinetic energy of that liquid due to its lower temperature. That is, in order to have the same freedom of motion (the same structure) the volume available to an argon atom must be sufficiently greater than that available to a xenon atom to overcome the greater freedom given the xenon by its higher thermal energy.

We had expected to publish a calculation of the potential curve for xenon from these data using the method of Hildebrand and Wood[11] as outlined by Hildebrand, Wakeham, and Boyd[12] but have decided to postpone this until the end of the war.

ACKNOWLEDGMENT

The junior author is deeply indebted to the E. I. du Pont de Nemours Company and to the Great Western Dow Chemical Company for fellowships which freed his time for the pursuit of this research.

[11] J. H. Hildebrand and S. E. Wood, J. Chem. Phys. **1**, 817 (1933).
[12] J. H. Hildebrand, H. R. R. Wakeham, and R. N. Boyd, J. Chem. Phys. **7**, 1094 (1939).

Photographic Development as a Catalyzed, Heterogeneous Reaction*

T. H. JAMES
Kodak Research Laboratories, Kodak Park Works, Rochester, New York

Development is considered as a catalyzed reaction which takes place at the interface between the silver nuclei and the solid silver halide crystal. Silver atoms formed at the interface may migrate along the silver surface for some distance before they become incorporated into the silver lattice. An explanation of filament formation is given on this basis.

FOLLOWING the lead of Luther and Leubner,[1] the writer carried out a series of investigations on the reactions of developing agents with silver salts under various experimental conditions. The general plan was to start with the simple reaction between silver ions and a developing agent in solution and then to add successive complicating factors in such a way that conditions prevailing during the actual development of a photographic image were approached, step by step. The execution of the program was greatly facilitated by the choice of hydroxylamine as the principal developing agent. A less complete investigation employing hydroquinone served as a check upon the hydroxylamine results.

The general results of the work with hydroxylamine may be summarized briefly. The reaction between the agent and silver ions in slightly acid solution is strongly catalyzed[2] by metallic silver. This catalyzed reaction yields exclusively nitrogen as the oxidation product of the hydroxylamine, and the rates of formation of silver coincide with the rates of evolution of the nitrogen (within the limits of experimental error). The mechanism of the catalysis involves primarily an adsorption of silver ions to the silver.[2,3] Reaction is between the adsorbed silver ions and the hydroxylamine ions, H_2NO^-. Adsorption of the latter is probably involved to a secondary degree. The reaction between silver ions and hydroquinone is entirely analogous, except that no evidence for the adsorption of the hydroquinone itself was observed.[4]

In alkaline solution, the catalyzed reaction again predominates when the silver-ion concentration is low. Increase in either silver-ion concentration or pH favors relatively an uncatalyzed reaction which yields nitrous oxide as the oxidation product.[5-7]

Slightly alkaline hydroxylamine reduces silver chloride largely by way of the catalyzed reaction.[8] Silver bromide in the presence of excess bromide ion is reduced almost entirely by way of the catalyzed reaction even in a moderately alkaline solution (pH = 10 − 11).[9] Increase in pH again relatively favors the uncatalyzed reaction. Both salts react in essentially the solid state. Exposure to light greatly increases the rate of reaction because the light forms silver nuclei which act as the initial catalysis centers. Exposure to light thus favors the catalyzed reaction. Adsorption of gelatin, bromide ions, and certain cyanine dyes to the surface of the silver salt likewise favors the catalyzed reduction relative to the uncatalyzed.[9,10]

The results of the kinetic studies indicate that, when silver nuclei are present, reduction proceeds at the solid interface along the line where the silver meets the silver halide. The silver ions at this interface are already subjected to adsorption forces, and are probably displaced somewhat from their normal lattice positions. The concentration of the activated complex, (H_2NO^-, Ag^+, S†), will depend upon the availability of the silver ions for combination with the (adsorbed) hydroxylamine ions,[11a] and thus will be influenced

* Communication No. 925 from the Kodak Research Laboratories.

[1] R. Luther and A. Leubner, Brit. J. Phot. **59**, 632 *et seq.* (1912).

[2] T. H. James, J. Am. Chem. Soc. **61**, 2379 (1939).

[3] T. H. James, J. Am. Chem. Soc. **62**, 3411 (1940).

[4] T. H. James, J. Am. Chem. Soc. **61**, 648 (1939).

[5] S. E. Sheppard and C. E. K. Mees, *Investigations of the Theory of the Photographic Process* (Longmans, Green, and Company, New York, 1907), p. 141 ff.

[6] M. L. Nichols, J. Am. Chem. Soc. **56**, 841 (1934).

[7] T. H. James, J. Am. Chem. Soc. **64**, 731 (1942).

[8] T. H. James, J. Am. Chem. Soc. **62**, 536, 1649 (1940).

[9] T. H. James, J. Chem. Phys. **10**, 464 (1942).

[10] T. H. James, J. Phys. Chem. **46**, 1068 (1942).

[11a] T. H. James and G. Kornfeld, Chem. Rev. **30**, 1 (1942).

by factors in addition to the silver-silver ion couple. The retarding action of extraneous adsorbed material, such as gelatin, would follow from the expected decrease in effective concentration of the complex. The relation of these results to previous theories of development has already been discussed,[11a] as well as an important secondary effect upon the kinetics of development exerted by the electric charge of the silver halide grain.[11a, b]

Data on the kinetics of development by hydroxylamine of a simple commercial photographic emulsion showed no points at variance with the preceding interpretation of the catalyzed reaction. These results will be published in detail elsewhere.

There remains the important question of the disposition of the silver formed in the reaction. The silver atoms obviously do not simply replace the silver ions in space along all crystal directions, since the dimensional requirements are not the same.* Apart from this, electron micrographs show an irregular and often decidedly filamentary structure for the reduced silver. This structure appears to be characteristic of chemical development (at least of silver bromide grains) and has been observed in development by several different agents.[12–14] In some instances, thin filaments project well beyond the boundaries of the original silver bromide grain. The ribbon-like appearance of the filaments is in contrast to the appearance of silver produced by heavy exposures to light or electron beams. Such silver shows no evidence of filamentary structure, and projections from the grain surface have a knob-like appearance. (In the paper by Hall and Schoen, compare Figs. 2, 3, 4, and 5 with Figs. 7, 8, 9, and 12.)

Jelley[15] has drawn attention to a significant feature of these filaments: "The pictures which they (Hall and Schoen) obtained indicate that development starts at certain preferred centers, presumably the latent image specks, and then spreads through the crystal." The filaments which form do not have parallel edges, but show frequent angular enlargements in the plane of the ribbon. These enlargements often take the form of flat, triangular crystals (several of which may be seen in micrographs reproduced in Jelley's paper). "This is a strong indication that the sides of the filaments correspond to the octahedral (111) faces of the silver crystals, so that the filaments may be considered as silver crystals which have grown chiefly in one dimension."

Electron micrographs of grains developed by hydroxylamine in connection with the present investigation show the characteristic filamentary structure. This fact is of special interest in view of the simplicity of composition of the hydroxylamine developer. The phenomenon observed by Jelley is quite prominent. Micrographs of partially developed grains are shown in Fig. 1.

In conversations with the writer, David Harker and S. E. Sheppard suggested that migration phenomena play a part in development. This suggestion appears to supply the missing step in the development mechanism. Migration of the newly formed silver atoms for some distance along the silver surface before they become incorporated into the crystal lattice not only appears highly probable, but offers a solution to certain difficulties which arise in the interface theory of development. In particular, such migration offers a mechanism for the formation of the filaments.

Migration of crystallizing material along the surfaces of crystals has been detected in experiments with diverse materials.[16a, b] Such migrations may cover distances much larger than any required by filament formation in photographic

[11b] S. E. Sheppard, "Colloid-Chemical Aspects of Photographic Development" in *Colloid Chemistry, Theoretical and Applied* (Jerome Alexander, Editor, Reinhold Publishing Company, New York), Vol. V.

* Dankov has pointed out [Comptes rendus Acad. Sci. U.R.S.S. **24**, 773 (1939)] that in one plane the silver atoms in metallic silver have almost the identical spacing as the silver ions in silver bromide, but a marked difference occurs in the plane normal to this. In the case of silver chloride, coincidence does not occur in even one plane.

[12] M. von Ardenne, Zeits. f. angew. Phot. **2**, 14 (1940).

[13] C. E. Hall and A. L. Schoen, J. Opt. Soc. Am. **31**, 281 (1941).

[14a] C. E. K. Mees, *The Theory of the Photographic Process* (The Macmillan Company, New York, 1942), pp. 143, 312, 313.

[14b] E. F. Burton and W. H. Kohl, *The Electron Microscope* (Reinhold Publishing Company, New York, 1942), p. 210.

[15] E. E. Jelley, J. Phot. Soc. Am. **8**, 283 (1942).

[16a] M. Volmer, *Kinetik der Phasenbildung* (Theodor Steinkopff, Dresden and Leipzig, 1939).

[16b] R. M. Barrer, *Diffusion in and through Solids* (The Macmillan Company, New York, 1941).

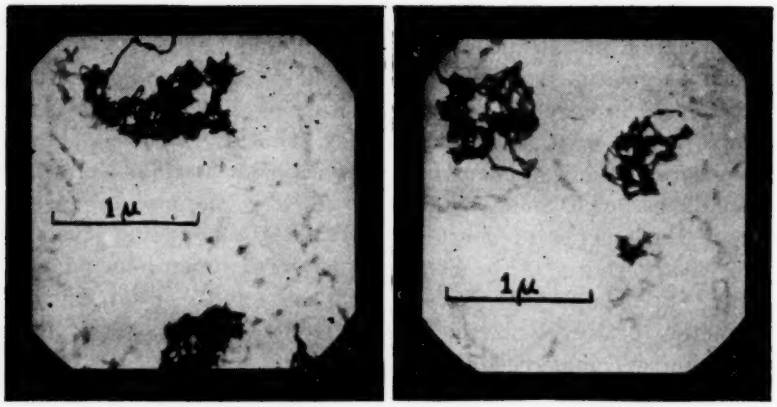

FIG. 1. Electron micrographs of grains developed by NH_2OH. Grains developed on specimen holder, and fixed. Note triangular crystals. (Micrographs by Norma Meyer and A. L. Schoen.)

development. Distinct filament formation during devitrification of fused masses of certain organic compounds has been described by Lehmann,[17a] and explained by Söllner[17b] on the basis of surface migration. Söllner applies the same general explanation to the formation of "hair-silver." *

Andrade[18] has shown that silver atoms making up the surfaces of thin silver films are mobile at temperatures as low as 250°C, or 700° below the melting point of massive silver. Migration of such surface atoms led to the formation of spherulites "with the (111) face parallel to the substrate, growing freely in a tangential direction, but adding atoms *normally to the last completed (111) face only with great reluctance*" (italics mine). The energy of activation of such migrations evidently is quite low, not exceeding a few thousand calories.[16b]

Howey[19] observed that thin, single-crystal needles of silver are formed under proper conditions by condensation of silver vapor upon drops of silver. The shape and crystalline orientations of the needles indicate that they result from growth occurring much more rapidly in a certain [110] direction than in other directions. Nuclei leading to such filamentary formation could start as rows of atoms having a stronger field of force at the end than along the sides. Atoms striking the sides would either evaporate again, or they would migrate along the surface and be incorporated into the lattice preferentially at the ends.

Let us return to the problem of reaction at the silver-silver halide interface. When a silver ion is reduced, the newly-formed silver atom for the moment is in an unstable position. The heat of the reaction is fairly high (cf. reference 14*a*, p. 314), probably 10,000 calories or more. (According to preliminary measurements by Zuev,[20] the heat of development of silver bromide by hydroquinone amounts to around 9,000 calories. Preliminary measurements by Lambert[21] indicate an even higher figure for hydroxylamine.) Calculations cited by Rabinovitch[20] make it quite unlikely that any significant heating of the silver

[17a] O. Lehmann, *Molekularphysik I* (1888), p. 715.

[17b] K. Söllner, Kolloid Zeits. **59**, 55 (1932).

* Hair-silver is most readily obtained by the reduction of silver sulfide in the temperature range of roughly 250–600°C. Kohlschütter [Zeits. f. Elektrochemie **38**, 345 (1932)], who has carried out extensive investigations on the phenomenon, assumes that at least a portion of the silver making up the fibers comes from *inside* the silver sulfide particles, so that the original silver nuclei are pushed out from the surface by the accumulating silver. The high mobility of silver ions through the silver sulfide at the temperatures involved would favor this process. Although such a mechanism may play a part in the formation of hair-silver on silver sulfide, Kohlschütter points out that it is hardly probable for the formation of hair-silver during the reduction of silver chloride, where the hair-silver was obtained only above the melting point of the chloride. The assumption that migration of interstitial silver ions within the silver halide crystal plays any major role in development is open to serious objections (references 11*a*, *b*).

[18] E. da C. Andrade, Trans. Faraday Soc. **31**, 1137 (1935).

[19] J. H. Howey, Phys. Rev. **55**, 578 (1939).

[20] A. J. Rabinovitch, A. N. Bogoyavlenski, and Y. S. Zuev, Acta Physicochimica **16**, 307 (1942).

[21] R. H. Lambert, private communication.

bromide crystal occurs during normal development, but the newly-formed silver atoms may easily acquire the energy needed for migration along the silver surface. With favorable initial orientation, the silver crystals thus grow in essentially the manner described by Andrade, Howey, and Jelley. In actual development, adsorption of gelatin or even of developing agent to the growing silver crystal is a possible factor influencing the ultimate course of the growth.

As development proceeds, microscopic pits may form around the growing nuclei, owing to elimination of bromide ions into the solution and to migration of reduced silver. Such ulceration of the crystal exposes silver bromide surfaces which are no longer protected by adsorbed gelatin, and hence are more susceptible than the normal gelatin-coated surface to a direct attack by the developer. New silver nuclei can thus arise, and grow catalytically in the same fashion as the original latent-image nuclei. Thus, although development may start at only a few points on the crystal surface, a much larger number of nuclei may form during development, and give rise to a larger number of filaments. The "seaweed" cluster often observed in the electron micrographs of developed grains is the result. The number and size of the filaments should depend both upon the nature of the developer and the character of the emulsion. A developer which attacks the exposed grain in many places and easily forms new centers by attack on freshly available unprotected surface will yield more and finer filaments than one which attacks at only a very few points and does not readily form new centers during development. These general expectations are in agreement with the available data. Again, a very small, unripened silver bromide crystal, such as a Lippmann grain, is not expected to yield many filaments with any developer. Actually, the Lippmann crystals normally are converted into single silver filaments whose lengths exceed by severalfold the diameters of the original crystals.

An interesting experiment in which orientation in "development" was produced independently of light action is cited by Dankov and Kochetkov.[22] A monocrystalline silver bromide film was split at liquid-air temperature along its (100) and (010) cleavage planes. "Deformation with a needle resulted in the formation of two mutually perpendicular cracks, coinciding with directions [100] and [010], besides the rosettes which corresponded to deformation at room temperature. One of the samples of AgBr monocrystalline film . . . was partly reduced with the usual developer. The photomicrograph of the section of this sample near the crack coinciding with the direction [100] on the AgBr crystal . . . (shows) that the silver crystal developed so that crystal axis [110] of the metallic silver coincided with axis [010] of the AgBr crystal."

[22] P. D. Dankov and A. A. Kochetkov, Comptes rendus Acad. Sci. U.R.S.S. **26**, 785 (1940).

Letters to the Editor

PROMPT publication of brief reports of important discoveries in physics may be secured by addressing them to this department. The closing date for this department is the third of the month. Because of the late closing date for the section no proof can be shown to authors. The Board of Editors does not hold itself responsible for the opinions expressed by the correspondents. Communications should not in general exceed 600 words in length.

The Investigation of the Mechanism of Chemical Reactions with Heavy Oxygen

A. E. BRODSKY, N. I. DEDUSSENKO, I. A. MAKOLKIN, AND G. P. MIKLUKHIN
Pissarjevsky's Institute of Physical Chemistry, Academy of Sciences of the Ukrainian SSR, Ufa, U.S.S.R.
May 28, 1943

THE mechanism of some typical organic reactions was ascertained using the heavy oxygen isotope, which was concentrated through the fractionation of water by Urey's method.[1]

I.

The Beckmann's rearrangement of benzophenoxime has been carried on in the presence of PCl_5 and of heavy water with an excess of O^{18}. The excess density due to this isotope was: $\Delta d = 110$, 102, and 101γ in three experiments. The benzanilide obtained was hydrogenated and yielded water with $\Delta d = 118$, 109, and 98γ. It was shown that no exchange of oxygen atoms occurred between benzanilide and water and that no reaction of benzanilide with PCl_5 with formation of the imide took place. Hence, in the Beckmann's rearrangement, the oxygen of the oxime is entirely replaced in the anilide by the oxygen of the water. Thus, this reaction proceeds through intermediary dehydration and hydration steps (for example, according to the scheme of Stieglitz[2]) but not through direct intramolecular transfer, as is usually assumed.[3]

II.

The acylation of ethyl alcohol with acetic anhydride was carried out by alcohol, enriched with O^{18}. This alcohol was obtained by fractionation of dried alcohol in the same column and gave, after hydration,* water with $\Delta d = 73\gamma$. The ester formed by the reaction gave, after hydration, water with $\Delta d = 37\gamma$, i.e., exactly half of the Δd of the water from alcohol. Thus, the ester takes one oxygen atom from the alcohol and the second from the anhydride:

$$CH_3CO\cdot OCOCH_3 + H\cdot OC_2H_5 = CH_3CO\cdot OC_2H_5 + CH_3COO\cdot H,$$

where the dots indicate the places of rupture and of formation of bonds. It must be pointed out, that for alcohol and ester, these places are the same as for saponification or esterification, but in acetic acid the bond is formed in another place, as by saponification.

III.

The alkaline fusion of sodium salts of benzene-, β-naphthalene-sulfonic acids and of β-anthraquinone-monosulphonic acid was carried out with sodium hydroxide, prepared by dissolving sodium in water with $\Delta d = 157\gamma$. The phenolates obtained gave, after hydration, water with $\Delta d = 126$, 127, and 127γ for the three reactions mentioned. The water directly formed by the fusion has $\Delta d = 120$, 125, and 75γ. It was ascertained that in the conditions of the fusion no isotopic exchange of oxygen atoms occurs between the sulphosalts or phenolates and water or NaOH. Thus, the alkaline fusion passes through elimination of SO_3Na and addition of ONa (the scheme of Voroshzow,[4] similar to the one of Wieland for sulphonation and nitration, seems to be the most trustworthy) but not through intermediate rearrangement of the sulphonic salts into salts of ethers of sulfonic acids: $RSO_3Na \rightarrow RO\cdot SO_3Na$ (as assumed by Bucherer[5]).

IV.

The xanthation of ethyl alcohol and of alkalicellulose with the same NaOH as in III gave water with the same $\Delta d = 155\gamma$ and xanthates which gave, after hydration, water with normal oxygen. Thus, by the xanthation, the oxygen passes from alkali into the water formed, according to the scheme:

$$RO\cdot H + HO\cdot Na + CS_2 = RO\cdot CS\cdot SNa + H_2O.$$

No appreciable isotopic exchange of oxygen atoms occurs between water and alcohol, cellulose, their xanthates or trialcoholate of cellulose, but alkalicellulose exchanges its oxygen atoms slowly with water. If no such exchange occurs in OH groups of alcoholates, all these results indicate that the alkalicellulose is an addition-product: $C_6H_{10}O_5\cdot NaOH$, with properties of a weak electrolyte: $C_6H_{10}O_5\cdot Na^+ + OH^-$; but not a compound of alcoholate type: $C_6H_9O_4\cdot ONa$, as is often assumed.

[1] Brodsky a. Scarre, Acta Physicochim. U.R.S.S. **10**, 728 (1939).
[2] Stieglitz, J. Am. Chem. Soc. **36**, 280 (1914); **44**, 407 (1922).
[3] Gilman, Org. Chem. **1**, 761–798 (1933).
* Editor's Note: The author evidently uses the word hydration here and subsequently to refer to the formation of water containing all the oxygen of the compound, for instance by the reaction $C_2H_5OH \rightarrow C_2H_4 + H_2O$.
[4] Voroshzow, Comptes rendus Acad. Sci. U.R.S.S. **1**, 107 (1940).
[5] Bucherer, Lehrb. d. Farbenchemie, 220 (1921).
[6] Gilman, Org. Chem. **2**, 1549 (1938).

THE AMERICAN INSTITUTE OF PHYSICS

INCORPORATED

ADMINISTRATIVE STAFF

HENRY A. BARTON, *Director*

MADELINE M. MITCHELL, *Publications Manager*

JOHN T. TATE, *Adviser on Publications*

Office: 175 Fifth Avenue, New York, New York

JOURNALS

THE PHYSICAL REVIEW
REVIEWS OF MODERN PHYSICS
JOHN T. TATE, *Editor (on leave)*
J. W. BUCHTA, *Acting Editor*

JOURNAL OF THE OPTICAL SOCIETY OF AMERICA
GEORGE R. HARRISON, *Editor*

THE JOURNAL OF THE ACOUSTICAL SOCIETY OF AMERICA
FLOYD A. FIRESTONE, *Editor*

AMERICAN JOURNAL OF PHYSICS
DUANE ROLLER, *Editor*

THE REVIEW OF SCIENTIFIC INSTRUMENTS
GAYLORD P. HARNWELL, *Editor*

THE JOURNAL OF CHEMICAL PHYSICS
JOSEPH E. MAYER, *Editor*

JOURNAL OF APPLIED PHYSICS
ELMER HUTCHISSON, *Editor*

GOVERNING BOARD

PAUL E. KLOPSTEG, *Chairman*
Central Scientific Company

GEORGE B. PEGRAM, *Secretary*
Columbia University

For the American Physical Society:

JOHN T. TATE
University of Minnesota

L. A. DUBRIDGE
University of Rochester

GEORGE B. PEGRAM
Columbia University

For the Optical Society:

A. C. HARDY
Massachusetts Institute of Technology

K. S. GIBSON
National Bureau of Standards

R. C. GIBBS
Cornell University

For the Acoustical Society of America:

HARVEY FLETCHER
Bell Telephone Laboratories

FLOYD A. FIRESTONE
University of Michigan

WALLACE WATERFALL
The Celotex Corporation

For the Society of Rheology:

R. B. DOW
Aberdeen Proving Ground

HERMANN MARK
Brooklyn Polytechnic Institute

N. W. TAYLOR
The Pennsylvania State College

For the American Association of Physics Teachers:

A. G. WORTHING
University of Pittsburgh

PAUL E. KLOPSTEG
Central Scientific Company

T. D. COPE
University of Pennsylvania

The American Institute of Physics is a membership corporation of which five societies are the founding members. These five societies are the principal national societies devoted to pure and applied physics in America. Their names, and those of their representatives who form the Governing Board of the Institute, are given above. The principal work of the Institute is the publication of journals sponsored by the societies or by itself. The names and the editors of the journals are also listed above.

The broad purpose of the Institute is to represent, in all matters of wide or common interest, the five thousand or more members and subscribers associated with the Founder Societies and the journals. It aims to advance the science and profession of physics, and to promote cooperation between pure research, the applied sciences and the industries. To achieve these aims, it is greatly in need of an endowment, and is empowered by law to administer grants and funds of any kind.

CONTENTS

THE JOURNAL OF CHEMICAL PHYSICS VOL. 11, No. 7 JULY, 1943

Raman Spectra of Hydrocarbons. III. Dimethylethane, Cyclobutane, and Dipentene . . . . . FORREST F. CLEVELAND 301

Low Velocity Scattering of H^+ and H_2^+ in Hydrogen . . . . . J. H. SIMONS, C. M. FONTANA, E. E. MUSCHLITZ, JR., AND S. N. JACKSON 307

Low Velocity Scattering of H_2^+ in Hydrogen. The Determination of Neutralization . . . . . J. H. SIMONS, C. M. FONTANA, H. T. FRANCIS, AND L. G. UNGER 312

Scattering of Low Velocity Hydrogen Ions in Water Vapor . . . . . J. H. SIMONS, H. T. FRANCIS, E. E. MUSCHLITZ, JR., AND G. C. FEYBURG 316

Scattering of Low Velocity Hydrogen Ions in Helium . . . . . J. H. SIMONS, E. E. MUSCHLITZ, JR., AND L. G. UNGER 322

Infra-Red Absorption of Palladium Vapor . . . JOHN TURKEVICH AND PETER COOPER STEVENSON 328

Structure of Liquid Mercury . . . . . J. A. CAMPBELL AND J. H. HILDEBRAND 330

Structure of Liquid Xenon . . . . . J. A. CAMPBELL AND J. H. HILDEBRAND 334

Photographic Sensitization as a Catalyzed, Heterogeneous Reaction . . . . . T. H. JAMES 338

Letters to the Editor:

Investigation of the Mechanism of Chemical Reactions with Heavy Oxygen . . . . . A. B. BRADLEY, N. I. SHEPHERDSON, I. A. MAKOLKIN AND G. P. MIKLUKHIN 343

LANCASTER PRESS, INC., LANCASTER, PA.